# Hepatoprotective Effect of Syringic Acid and Vanillic Acid on CCl4-Induced Liver Injury

Ayano Itoh,[a] Katsuhiro Isoda,[a] Masuo Kondoh,[a] Masaya Kawase,[a] Akihiro Watari,[a] Masakazu Kobayashi,[b] Makoto Tamesada,[b] and Kiyohito Yagi*,[a]

[a] Graduate School of Pharmaceutical Sciences, Osaka University; 1–6 Yamada-oka, Suita, Osaka 565–0871, Japan: and [b] Research and Development Center, Kobayashi Pharmaceutical Co., Ltd.; 1–30–3 Toyokawa, Ibaraki, Osaka 567–0057, Japan.        Received December 22, 2009; accepted March 16, 2010; published online March 19, 2010

The mycelia of the edible mushroom *Lentinula edodes* can be cultured in solid medium containing lignin, and the hot-water extracts (L.E.M.) is commercially available as a nutritional supplement. During the cultivation, phenolic compounds, such as syringic acid and vanillic acid, were produced by lignin-degrading peroxidase secreted from *L. edodes* mycelia. Since these compounds have radical scavenging activity, we examined their protective effect on oxidative stress in mice with CCl4-induced liver injury. We examined the hepatoprotective effect of syringic acid and vanillic acid on CCl4-induced chronic liver injury in mice. The injection of CCl4 into the peritoneal cavity caused an increase in the serum aspartate aminotransferase (AST) and alanine aminotransferase (ALT) levels. The intravenous administration of syringic acid and vanillic acid significantly decreased the levels of the transaminases. Four weeks of CCl4 treatment caused a sufficiently excessive deposition of collagen fibrils. An examination of Azan-stained liver sections revealed that syringic acid and vanillic acid obviously suppressed collagen accumulation and significantly decreased the hepatic hydroxyproline content, which is the quantitative marker of fibrosis. Both of these compounds inhibited the activation of cultured hepatic stellate cells, which play a central role in liver fibrogenesis, and maintained hepatocyte viability. These data suggest that the administration of syringic acid and vanillic acid could suppress hepatic fibrosis in chronic liver injury.

**Key words**   hepatoprotection; *Lentinula edodes*; syringic acid; vanillic acid; polyphenol

The edible mushroom *Lentinula edodes* (shiitake) contains bioactive compounds that have immune-modulating, antitumor, antibacterial, antiviral, and antiparasitic effects.[1—4] The mycelia of *L. edodes* can be cultured in solid medium, and the hot-water extract (L.E.M.) is commercially available as a nutritional supplement. The main components of L.E.M. are sugars, proteins, and polyphenolic compounds. Polyphenols have protective effects against cancers, cardiovascular disease, and neurodegenerative disorders.[5—7] Among polyphenols, syringic acid and vanillic acid are enriched in the solid medium of cultured *L. edodes* mycelia.[8] *L. edodes* grown in lignocellulose secretes lignin-degrading peroxidase into the culture medium.[9] The mycelia-derived enzymes degrade the lignin to produce phenolic compounds, particularly syringic acid and vanillic acid. In our previous study, we demonstrated that these phenolic compounds had a hepatoprotective effect on concanavalin A (ConA)-induced liver injury in mice.[8] We intraperitoneally injected syringic acid or vanillic acid into mice shortly before a ConA injection into the tail vein, which greatly increased the levels of serum aspartate aminotransferase (AST) and alanine aminotransferase (ALT). In addition, the inflammatory cytokines tumor necrosis factor (TNF)-$\alpha$, interferon-$\gamma$ (IFN-$\gamma$), and interleukin (IL)-6 in the serum increased rapidly, within 3 h of the ConA administration. The administration of syringic acid or vanillic acid significantly decreased the transaminase and inflammatory cytokine levels and suppressed the disorganization of the hepatic sinusoids. Since ConA-induced liver injury is a mouse model of immune-mediated liver injury that resembles viral and autoimmune hepatitis in humans, the phenolics appeared to have immunomodulating activity.

Polyphenols act as antioxidants by scavenging reactive oxygen species (ROS), which produce oxidative stress and can adversely affect many cellular processes. In the present study, we examined the possible hepatoprotective effects of two phenolic compounds, syringic acid and vanillic acid, on oxidative stress in chronic CCl4-induced liver injury in mice. We found that both phenolic compounds could suppress oxidative damage, especially liver fibrosis caused by repeated administration of CCl4.

## MATERIALS AND METHODS

**Reagents**   Syringic acid, vanillic acid, and CCl4 were purchased from WAKO Pure Chemicals, Co., Ltd. (Osaka, Japan). The chemical structures of syringic acid and vanillic acid were shown in Fig. 1. L.E.M. was obtained from Kobayashi Pharmaceutical Co., Ltd. (Osaka, Japan). CCl4 was dissolved in olive oil, and L.E.M., syringic acid, and vanillic acid were dissolved in phosphate buffered saline (PBS) for administration into mice. L.E.M., syringic acid, and vanillic acid were dissolved in culture medium for hepatocytes or hepatic stellate cells for *in vitro* experiments.

**Animals**   BALB/c mice and Sprague-Dawley rats were purchased from SLC (Shizuoka, Japan). The animals were housed in an air-conditioned room at 22 °C before the experiment. The animal experiments were conducted according to the ethical guidelines of Osaka University Graduate School
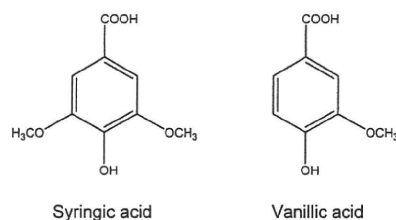


Fig. 1.   Chemical Structures of Syringic Acid and Vanillic Acid

of Pharmaceutical Sciences. The experimental protocol was submitted to the Committee on the Guidelines for Animal Experiments in Graduate School of Pharmaceutical Sciences, and the experiments were conducted after gaining the approval. Mice in the chronic liver injury model received intraperitoneal injections of $CCl_4$ (0.5 ml/kg body weight) and intravenously administered L.E.M., syringic acid, or vanillic acid (10 mg/kg body weight) twice a week for 4 weeks. Twenty-four hours after the L.E.M., syringic acid, or vanillic acid injection, the mice were anesthetized. Then, blood samples were collected to determine the transaminase activity, and the livers were excised for Azan staining and determination of hydroxyproline and malondialdehyde.

**Assays** Serum AST and ALT levels were measured by using an assay kit (Transaminase C-II, WAKO, Osaka, Japan).

**Histological Analysis** Liver specimens were fixed in 4% paraformaldehyde and embedded in paraffin. Sections were cut from the tissue blocks and mounted on slides. Azan staining was then performed to evaluate the extent of liver fibrosis.

**Measurement of Hydroxyproline Content** Hepatic hydroxyproline content was measured by using Kivirikko's method[10] with some modifications. Briefly, liver tissue (50 mg) was hydrolyzed with 6 mol/l HCl at 110 °C for 24 h in a glass test tube. After centrifugation at 3000 rpm for 10 min, 2 ml of the supernatant was neutralized with 8 N KOH. Two grams of KCl and 1 ml of 0.5 mol/l borate buffer were then added to the neutralized supernatant, followed by a 15-min incubation at room temperature and then a 15-min incubation at 0 °C. Freshly prepared chloramine-T solution was then added, and the sample was incubated at 0 °C for 1 h, followed by the addition of 2 ml of 3.6 mol/l sodium thiosulfate. The samples were incubated at 120 °C for 30 min. Then, 3 ml of toluene was added, and the samples were incubated for 20 min at room temperature. After centrifugation at 2000 rpm for 5 min, 2 ml of the supernatant was added to 0.8 ml buffer containing Ehrlich's reagent and incubated for 30 min at room temperature. The samples were then transferred to a plastic tube, and the absorbance was measured at 560 nm. The hydroxyproline content was expressed as micrograms of hydroxyproline per gram of liver.

**Measurement of Malondialdehyde** Lyophilized liver tissue (25 mg) was boiled for 30 min in a solution containing 250 ml of 1.15% KCl, 150 ml of 1% $H_3PO_4$, and 500 ml of 0.67% thiobarbituric acid. Two milliliters of $n$-butanol was added to the ice-chilled sample, and then the sample was stirred for 30 min. After centrifugation at $3000 \times g$ for 10 min, the upper $n$-butanol phase was collected, and the amount of malondialdehyde was colorimetrically determined at 535 and 520 nm.

**Isolation and Culture of Hepatic Stellate Cells** Hepatic stellate cells (HSCs) were isolated from 10-week-old male Sprague-Dawley rats by digesting the liver with Pronase-E (Merck Darmstadt, Germany) and collagenase type I (WAKO Pure Chemicals Co., Osaka, Japan) as previously described.[11] Isolated HSCs were seeded at a density of $2 \times 10^5$ cells/cm$^2$ onto 24-well polystyrene culture plates (Asahi Techno Glass, Funabashi, Chiba, Japan) to observe the morphology and analyze fibrosis-related gene expression. Cells were cultured in Dulbecco's modified Eagle's medium

(Sigma, St. Louis, MO, U.S.A.) supplemented with 10% fetal bovine serum.

**Isolation and Culture of Hepatocytes** Hepatocytes were isolated from male BALB/c mice by perfusing the liver with collagenase, according to the method of Seglen.[12] Cells were seeded at a density of $1 \times 10^5$ cells/cm$^2$ into multi-well culture plates pre-coated with collagen type I (Asahi Techno Glass, Funabashi, Chiba, Japan). The basal medium consisted of 50 U/ml penicillin G, 50 $\mu$g/ml streptomycin (ICN Biochemicals, Inc., Costa Mesa, CA, U.S.A.), 1 $\mu$M insulin, 1 $\mu$M dexamethasone (WAKO Pure Chemicals Co., Osaka, Japan), and 10% fetal bovine serum in William's medium E (MP Biomedicals, Inc., Kayserberg, France). Six hours after the cells were seeded, the basal medium was replaced with medium containing L.E.M., syringic acid, or vanillic acid at a final concentration of 1.0 mg/ml without insulin and dexamethasone. Cells were then cultured for 24—48 h, and viable cells were counted after trypan blue staining.

**Reverse Transcription-Polymerase Chain Reaction (RT-PCR)** The HSCs were cultured for 7 d and the total RNA was extracted using High Pure RNA Isolation Kit (Roche, Mannheim, Germany). The gene expression of collagen 1 $\alpha$(I) was analyzed using the following primers: forward 5′-TGCCGTGACCTCAAGATGTG-3′ and reverse 5′-CACAAGCGTGCTGTAGGTGA-3′. The gene expression of a smooth muscle actin ($\alpha$-SMA) was analyzed using the following primers: forward 5′-CCGAGATCTCACCGACTACC-3′ and reverse 5′-TCCAGAGCGACATAGCACAG-3′. The gene expression of $\beta$-actin was analyzed using the following primers: forward 5′-CCCAGAGCAAGAGAGGCATC-3′ and reverse 5′-CTCAGGAGGAGCAATGATCT-3′.

The RT-PCR was examined using RNA PDR Kit (TaKaRa, Kyoto, Japan).

**Statistical Analysis** The data were analyzed for statistical significance by using Student's $t$-test and Dunnett's test.

## RESULTS

**Effect on $CCl_4$-Induced Chronic Liver Injury** We examined the hepatoprotective effect of syringic acid and vanillic acid on $CCl_4$-induced chronic liver injury in mice. As shown in Fig. 2, after 4 weeks of $CCl_4$ treatment, the activities of blood AST and ALT increased 30-fold and 127-fold, respectively, compared with controls. The intravenous administration of syringic acid or vanillic acid significantly decreased the activities of AST and ALT. These results suggest that syringic acid and vanillic acid suppress the hepatic inflammation caused by repeated $CCl_4$ treatments. We also examined the effect of syringic acid and vanillic acid on liver fibrogenesis. Figure 3 shows typical Azan staining results, in which fibrous materials are stained blue. In the controls (Fig. 3A), hardly any blue staining was observed in the pericentral area. In contrast, the livers injured by chronic $CCl_4$ treatment displayed a considerable accumulation of fibrous materials (Fig. 3B). $CCl_4$ treatment for 4 weeks caused an excessive deposition of collagen fibrils that was sufficient for the evaluation of the antifibrogenic effect of syringic acid and vanillic acid. Based on the results of Azan staining, the syringic acid and vanillic acid treatments obviously suppressed collagen accumulation (Figs. 3D, E). To quantitatively evaluate the effect of syringic acid and vanillic acid on fibrogenesis, we
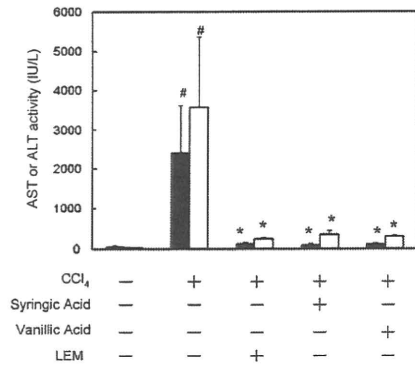
**Fig. 2.** Effect of Syringic Acid and Vanillic Acid on CCl₄-Induced Chronic Hepatic Injury

Mice received an intraperitoneal injection of CCl₄ and an intravenous injection of L.E.M., syringic acid, or vanillic acid twice a week for 4 weeks. The serum levels of AST (solid column) and ALT (open column) were determined. The values are mean±S.D ($n=4$). The data were analyzed by Student's $t$-test ($\#p<0.05$, as compared to uninjured control mice) and Dunnett's method ($*p<0.05$, as compared to CCl₄-injured control mice).
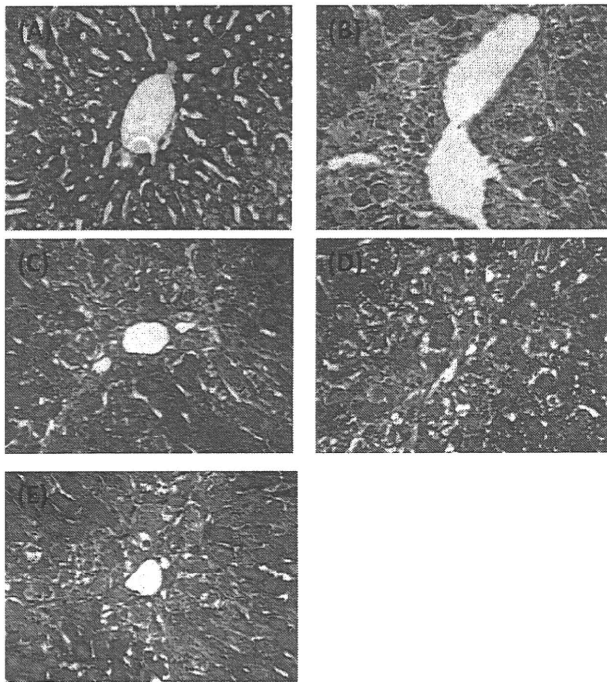


**Fig. 3.** Azan Staining of Liver Sections

Livers were excised from normal mice (A), CCl₄-injured control mice (B), L.E.M.-treated mice (C), syringic acid-treated mice (D), and vanillic acid-treated mice (E). Original magnification ×400.



**Fig. 4.** Effect of Syringic Acid and Vanillic Acid on the Hydroxyproline Content of the Liver

The hydroxyproline content of the liver was measured after 4 weeks of treatments. The values are mean±S.D. ($n=4$). The data were analyzed by Student's $t$-test ($\#\#p<0.01$, as compared to uninjured control mice) and Dunnett's method ($*p<0.05$, as compared to CCl₄-injured control mice).



**Fig. 5.** Effect of Syringic Acid and Vanillic Acid on the Suppression of Oxidative Stress

The malondialdehyde content of the liver was determined after 4 weeks of experiments. The values are mean±S.D. ($n=4$). The data were analyzed by Student's $t$-test ($\#\#p<0.01$, as compared to uninjured control mice) and Dunnett's method ($*p<0.05$, as compared to CCl₄-injured control mice).

measured the hepatic hydroxyproline content, which parallels the extent of fibrosis. After 4 weeks of CCl₄ treatment, the hepatic hydroxyproline content increased 4.6-fold as compared with the controls (Fig. 4). The intravenous administration of syringic acid or vanillic acid significantly decreased the hepatic hydroxyproline content. These data suggest that syringic acid and vanillic acid can suppress hepatic fibrosis in chronic liver injury. Next, we measured the amount of malondialdehyde in the liver samples as a marker of oxidative stress. The malondialdehyde content was drastically increased after 4 weeks of CCl₄ treatment, but the intravenous administration of syringic acid or vanillic acid significantly
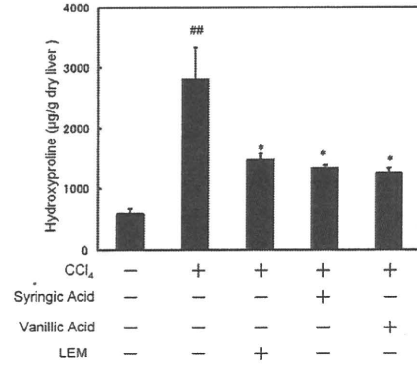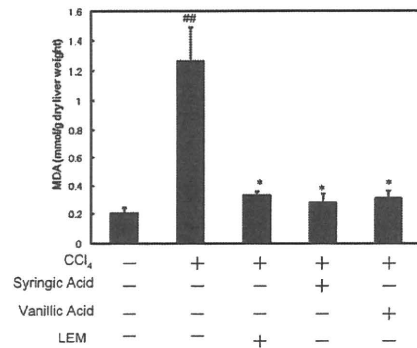
decreased the malondialdehyde content to an almost normal level (Fig. 5). The protective effects of syringic acid and vanillic acid were almost comparable to that of L.E.M. (Figs. 2—5).

**In Vitro Effect on HSC Activation and Hepatocyte Viability** We examined the direct effect of syringic acid and vanillic acid on the activation of HSCs, which play a central role in liver fibrogenesis, using the monolayer culture. HSCs are activated during the monolayer culture to transform into proliferating myofibroblast-like cells. As shown in Fig. 6A, HSCs were activated after 7 d of culture to be fibroblastic cell-type. The addition of syringic acid or vanillic acid dose-dependently suppressed the activation (Fig. 6B). HSCs maintained their quiescent state by the addition of more than 0.5 mg/ml of the respective compound. Next, the effect of syringic acid and vanillic acid on gene expression of Type I collagen and α-SMA, which are markers of activated HSCs, was examined. HSCs were cultured for 7 d in the presence or absence of syringic acid or vanillic acid, and the gene expression was analysed by RT-PCR. As shown in Fig. 7, syringic acid and vanillic acid remarkably suppressed the expression of collagen and α-SMA genes, indicating that the phenolic compounds directly act on HSCs and suppress the activation
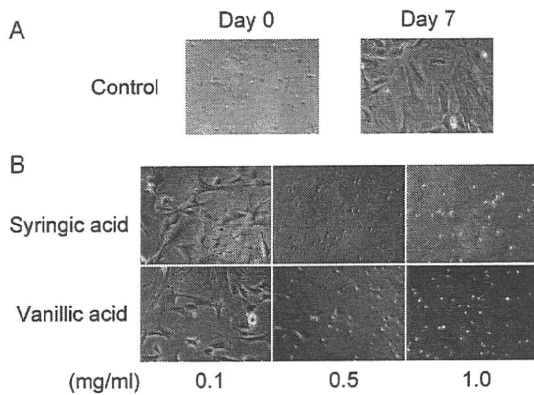
Fig. 6.　Phase-Contrast Micrographs of Cultured HSCs

Freshly isolated HSCs were cultured for 7 d in the absence (A) and presence (B) of syringic acid or vanillic acid at the indicated concentration. Original magnification ×200.
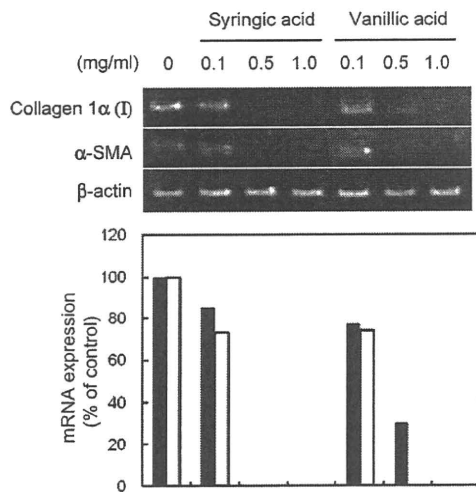


Fig. 7.　RT-PCR Analysis of Gene Expression Relating to HSC Activation

Bottom figure shows the relative expression of collagen 1 $\alpha$(I) (closed bar) and $\alpha$-SMA (open bar) compared with the non-addition control.
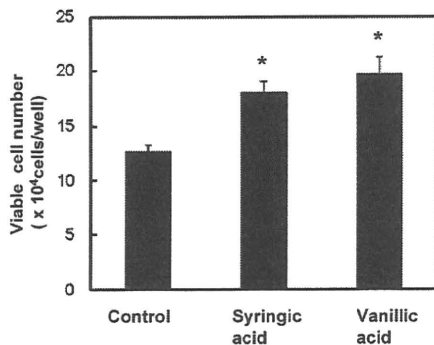


Fig. 8.　Effect of Syringic Acid and Vanillic Acid on Viability of Cultured Hepatocytes

Freshly isolated hepatocytes were cultured for 24 h in the absence or presence of 1.0 mg/ml syringic acid or vanillic acid. Viability was measured by trypan blue exclusion test. The data were analyzed by Dunnett's method ($*p<0.05$, as compared to control).

to maintain the quiescent state. We then examined the effect of the compounds on liver parenchymal hepatocytes using the primary culture (Fig. 8). Hepatocytes were isolated and cultured in the presence or absence of syringic acid or vanil-

lic acid. After 24 h of culture, viable cells were counted using trypan blue exclusion test. The addition of syringic acid or vanillic acid significantly maintained viability of cultured hepatocytes. These results suggested that syringic acid or vanillic acid might suppress liver fibrogenesis and inflammation by inhibiting HSC activation and protecting hepatocytes, respectively in chronically liver injured mice.

## DISCUSSION

The physiological functions of plant-derived phenolic compounds have been extensively reported.[7,13,14] Syringic acid and vanillic acid possess antimicrobial, anti-cancer, and anti-DNA oxidation properties.[15—17] We recently found that syringic acid and vanillic acid could act as immunomodulators in mice with ConA-induced liver injury.[8] In the present study, we show that syringic acid and vanillic acid have protective effects in mice with $CCl_4$-induced liver injury. Both phenolic compounds dramatically suppressed liver fibrogenesis in the chronic $CCl_4$-treatment model. When these phenolics are orally administered to hamsters, they are adsorbed and appear in the blood within 40 min.[18] Although these compounds are intravenously administered in the present study, oral administration could also elicit the hepatoprotective effect. The syringic acid and vanillic acid contents in L.E.M. are 450 and 378 $\mu$g/g, respectively. Thus, the contents are relatively small, but these compounds are commercially available at low prices. Therefore, syringic acid and vanillic acid might be promising oral agents for the prevention of liver disease.

We evaluated the hepatoprotective effect of phenolic compounds in mice with $CCl_4$-induced liver injury. After intravenous administration, $CCl_4$ is introduced into the liver, where it is toxic to hepatocytes. Cytochrome P-450 in the endoplasmic reticulum of hepatocytes catalyzes the dehalogenation to produce an unstable complex trichloromethyl radical,[19] resulting in the extensive necrosis of hepatocytes that leads to liver inflammation. In the present study, the transaminase level in the serum was drastically increased by $CCl_4$ treatment. Generation of ROS degrade polyunsaturated lipids to form malondialdehyde, which is a marker of oxidative stress. The chronic $CCl_4$ treatment significantly increased the malondialdehyde content of the liver. Syringic acid and vanillic acid clearly suppressed the transaminase and malondialdehyde levels in $CCl_4$-treated mice. Since both of these compounds have 1,1-diphenyl-2-picrylhydrazyl (DPPH) radical scavenging activity,[8] the suppression of ROS generation appears to be responsible for the hepatoprotective effect. Moreover, the $CCl_4$-induced liver fibrogenesis was suppressed by the administration of syringic acid and vanillic acid. The activation of HSCs is responsible for the development of liver fibrosis.[20,21] During liver injury with persistent inflammation, HSCs are activated to differentiate into proliferating myofibroblast-like cells and overproduce extracellular matrix, leading to fibrogenesis. Since HSCs are activated spontaneously during cell culture,[22] we examined the effect of syringic acid and vanillic acid on the activation of primary cell cultures of rat HSCs. Both of these compounds clearly inhibited the change from spherical to spindle shape and the expression of $\alpha$-smooth muscle actin and collagen Type I$\alpha$ genes, which are the markers of HSC activation. We also

examined the effect of syringic acid and vanillic acid on the maintenance of hepatocyte viability *in vitro*. Both of these compounds significantly maintained the viability of primary cell cultures of hepatocytes. Thus, syringic acid and vanillic acid could directly exert a physiological effect on hepatocytes and HSCs. Both phenolic compounds might affect $CCl_4$ metabolism to inhibit the generation of cytotoxic trichloromethyl radical in the liver. However, the direct effects of syringic acid and vanillic acid on HSCs and hepatocytes were shown in this study, and the protective effect was also shown in ConA-induced liver injured mice in our previous study.[8] Moreover, these phenolic compounds have strong radical scavenging activity. These results suggest that during the repeated treatment of $CCl_4$, these compounds could protect hepatocytes and HSCs from $CCl_4$-induced oxidative stress to suppress liver inflammation and fibrogenesis.

The hot-water extracts from cultured mycelia of *L. edodes* have versatile physiological effects and might contain promising seed compounds for pharmaceutical development. We have shown that syringic acid and vanillic acid have anti-oxidative and immunomodulating activities. In addition to these phenolics, L.E.M. could contain novel compounds with pharmaceutical potential. We are currently trying to isolate bioactive components from L.E.M.

## REFERENCES

1) Wasser S. P., Weis A. L., *Crit. Rev. Immunol.*, **19**, 65—96 (1999).
2) Suzuki H., Okubo A., Yamazaki S., Suzuki K., Mitsuya H., Toda S., *Biochem. Biophys. Res. Commun.*, **160**, 367—373 (1989).
3) Yamamoto Y., Shirono H., Kono K., Ohashi Y., *Biosci. Biotechnol. Biochem.*, **61**, 1909—1912 (1997).
4) Yamada T., Oinuma T., Niihashi M., Mitsumata M., Fujioka T., Hasegawa K., Nagaoka H., Itakura H., *J. Atheroscler. Thromb.*, **9**, 149—156 (2002).
5) Aggarwal B. B., Kumar A., Bharti A. C., *Anticancer Res.*, **23**, 363—398 (2003).
6) Aviram M., Dornfeld L., Kaplan M., Coleman R., Gaitini D., Nitecki S., Hofman A., Rosenblat M., Volkova N., Presser D., Attias J., Hayek T., Fuhrman B., *Drugs Exp. Clin. Res.*, **28**, 49—62 (2002).
7) Levites Y., Weinreb O., Maor G., Youdim M. B., Mandel S., *J. Neurochem.*, **78**, 1073—1082 (2001).
8) Itoh A., Isoda K., Kondoh M., Kawase M., Kobayashi M., Tamesada M., Yagi K., *Biol. Pharm. Bull.*, **32**, 1215—1219 (2009).
9) Forrester I. T., Grabski A. C., Mishra C., Kelley B. D., Strickland W. N., Leatham G. F., Burgess R. R., *Appl. Microbiol. Biotechnol.*, **33**, 359—365 (1990).
10) Kivirikko K. I., Laitinen O., Prockop D. J., *Anal. Biochem.*, **19**, 249—255 (1967).
11) Kawada N., Tran-Thi T. A., Klein H., Decker K., *Eur. J. Biochem.*, **213**, 815—823 (1993).
12) Seglen P. O., *Methods Cell Biol.*, **13**, 29—83 (1976).
13) Gao X., Xu Y. X., Janakiraman N., Chapman R. A., Gautam S. C., *Biochem. Pharmacol.*, **62**, 1299—1308 (2001).
14) Aggarwal S., Ichikawa H., Takada Y., Sandur S. K., Shishodia S., Aggarwal B. B., *Mol. Pharmacol.*, **69**, 195—206 (2006).
15) Aziz N. H., Farag S. E., Mousa L. A., Abo Zaid M. A., *Microbios*, **93**, 43—54 (1998).
16) Guimaraes C. M., Giao M. S., Martinez S. S., Pintado A. I., Pintado M. E., Bento L. S., Malcata F. X., *J. Food Sci.*, **72**, C039—C043 (2007).
17) Kampa M., Alexaki V. I., Notas G., Nifli A. P., Nistikaki A., Hatzoglou A., Bakogeorgou E., Kouimtzoglou E., Blekas G., Boskou D., Gravanis A., Castanas E., *Breast Cancer Res.*, **6**, R63—R74 (2004).
18) Chen C. Y., Milbury P. E., Kwak H. K., Collins F. W., Samuel P., Blumberg J. B., *J. Nutr.*, **134**, 1459—1466 (2004).
19) Castillo T., Koop D. R., Kamimura S., Triadafilopoulos G., Tsukamoto H., *Hepatology*, **16**, 992—996 (1992).
20) Albanis E., Friedman S. L., *Clin. Liver Dis.*, **10**, 821—833 (2006).
21) Friedman S. L., *Toxicology*, **254**, 120—129 (2008).
22) Sato M., Suzuki S., Senoo H., *Cell Struct. Funct.*, **28**, 105—112 (2003).

# 肝細胞機能制御を目的とした新規培養システムの開発

八木清仁, * 川瀬雅也, *a* 磯田勝広, *b* 近藤昌夫

# Development of Novel Culture System for Regulation of Hepatocyte Function

Kiyohito YAGI,* Masaya KAWASE,*a* Katsuhiro ISODA,*b* and Masuo KONDOH

*Graduate School of Pharmaceutical Sciences, Osaka University,*
*1-6 Yamada-oka, Suita, Osaka 565-0871, Japan*

Cultured hepatocytes are expected to be used for drug screening and bioartificial liver. Since hepatocytes lose their functions very rapidly *in vitro*, many attempts have been made to maintain their viability and functions. First, we want to introduce the surface modification of culture substrate using a starburst dendrimer. Addition of fructose to the terminal of the dendrimer was shown to be effective in maintianing hepatocyte function. As the second topic, we will show results of the use of a three-dimensional carrier for hepatocyte cultivation. Hepatocytes and bone marrow stromal cells were cocultured in silane beads, and packed into a radial flow-type bioreactor. The perfusion culture showed the effectiveness of bone marrow stromal cells for the maintenance of hepatocyte function. The next topic will be the trial of adenoviral gene transfer into hepatocytes. Thioredoxin gene was chosen because the products play important roles in redox control and antiapoptosis. The introduction of the gene could inhibit apoptosis and maintain the hepatocyte viability. Finally, we want to introduce the results on differentiation of stem cells into hepatocytes, because it is very difficult to obtain sufficient number of human hepatocytes. Human mesenchymal stem cells were cultured in the presence of several protein factors and the hepatocyte-specific marker was expressed after 2 weeks of induction culture. The use of human stem cells could be an important strategy for the support of a drug development system.

Key words——dendrimer; hepatocyte; radial flow-type bioreactor; mesenchymal stem cell

## 1. はじめに

培養肝細胞は医薬品開発のスクリーニング系やバイオ人工肝臓への応用が期待されているがその機能は viability の低下に伴い急速に消失していくため，機能維持を目的とした研究が活発に行われている．本総説ではこれまで我々が検討してきた培養基材の表面修飾，3次元培養，遺伝子導入，肝細胞の分化誘導について紹介する．足場依存性の細胞は培養基材の性質によって viability が著しく変動することが知られており，機能維持の成否は優れた培養基材の開発に依存していると言っても過言ではない．そこで機能性材料として注目されている樹木状

大阪大学大学院薬学研究科（〒565-0871 吹田市山田丘1-6）
現所属：*a*長浜バイオ大学バイオサイエンス学科（〒526-0829 長浜市田村町1266），*b*帝京平成大学薬学部（〒290-0193 市原市潤井戸2289）
*e-mail: yagi@phs.osaka-u.ac.jp
本総説は，日本薬学会第129年会シンポジウムS24で発表したものを中心に記述したものである．

高分子デンドリマーを用いた基材表面修飾の検討において，デンドリマーの末端にフルクトースを付加すると培養肝細胞の生存性，機能が良好に維持されたことを示す．また培養用ディッシュを用いた2次元培養では応用範囲が限られるため培養工学的検討として多孔性担体を用いた3次元培養の試みを紹介する．さらに細胞を接着させた3次元担体をラジアルフロー型バイオリアクターに充填し灌流培養を行った検討において，肝細胞と骨髄間質細胞との共培養が機能維持に効果的であったことを示す．次に遺伝子工学的アプローチとしてアデノウィルスベクターを用いてチオレドキシン遺伝子を導入することにより，肝細胞のアポトーシスを制御することが可能であったことを紹介する．最後に，細胞源に関する検討として再生医工学的アプローチによりヒト由来間葉系幹細胞を肝細胞へ誘導する試みを紹介し創薬支援システムへの応用について考察したい．

## 2. 機能性培養基材による肝機能制御
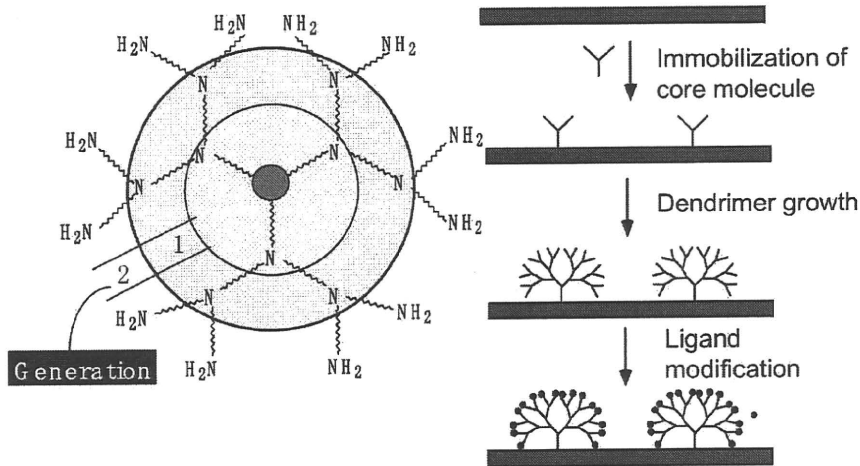
1985 年に Tomalia らによって報告されたデンド

Fig. 1. Structure of Polyamidoamine Dendrimer and Application for Cell Culture

リマーは樹木状多分岐高分子であり,[1]様々な領域でその応用が検討されている．直径は約数十 nm の分子であり，Fig. 1 で示すように，中心部分のコア，骨格分子，末端アミノ基から構成され，正確な分子設計が可能である．デンドリマーは規則的な枝分かれ構造を有する分子で，中心のコア分子から，段階的に伸長反応を行うことで枝分かれ数を増加させることができる．また，伸長反応を繰り返すことにより最外部の密度が高くなり，内部の密度が低くなっている．Figure 1 に示すようなポリアミドアミンデンドリマーは末端アミノ基部分の外表面が正に帯電しており，反応性が高い特徴を有している．このような特徴を活かして，様々な分野でデンドリマーの研究が行われている．[2-5] 医療分野へのデンドリマーの応用としては，内部の密度が粗であることを利用して，デンドリマー内部に薬物や遺伝子の封入，また外部の反応性の高さを利用して外部固定を行っている．デンドリマーにアンチセンス遺伝子を導入，またデンドリマー外部に薬物を固定化することによる薬物の徐放化の検討も行われている．

このようなデンドリマーの特徴を活かし，筆者らはデンドリマーにリガンド分子を結合させ，肝細胞培養基材とする方法を考案した．Figure 2 に示すようにカリウム tert-ブトキシドを用い基材表面にヒドロキシル基を導入し，グルタルアルデヒドを介してデンドリマーの固定化を行った．世代増加反応はこの反応を繰り返すことにより行い，最後に末端アミノ基へリガンド分子を結合させた．

筆者らはこれまでにキトサンゲル上で肝実質細胞を培養することに成功しており，特にキトサンの分子内アミノ基をフルクトースにより修飾したフルクトースキトサン上では未修飾のキトサンゲルよりも多くの細胞が接着し，肝特異的機能を維持することを報告した．そこでフルクトースに注目し，フルクトースをリガンドとしたフルクトースデンドリマーについて検討した．細胞非接着性のポリスチレンプレートにデンドリマーを固定化し，リガンドとしてフルクトースを修飾した．その結果，デンドリマーの世代数増加に伴い，修飾されたフルクトースも増加することを確認した．フルクトースデンドリマー上で数日培養を行うと成長因子などの添加なしに，細胞が高機能化すると言われるスフェロイド（球状組織体）を形成した．[6] しかし，ここではスフェロイドの接着性が弱く，さらに接着性を上げる必要が生じた．そこで，リガンドとしてフルクトースと，肝細胞表面に存在するアシアロ糖タンパクレセプターのリガンドとなるガラクトースの混合溶液をリガンド溶液とし，共固定した F/G デンドリマーを用いたところ，スフェロイドの接着が維持された．この，F/G デンドリマー上で培養したラット初代

八木清仁

大阪大学大学院薬学研究科教授．1981年大阪大学大学院博士後期課程修了（薬学博士）．1982–1984 年米国メリーランド大薬学部，NIH（NIEHS）で博士研究員として勤務．1983 年大阪大学薬学部助手．1992 年同助教授，2000 年3 月より現職．現在 C 型肝炎など肝疾患を対象とした創薬研究に取り組んでいる．
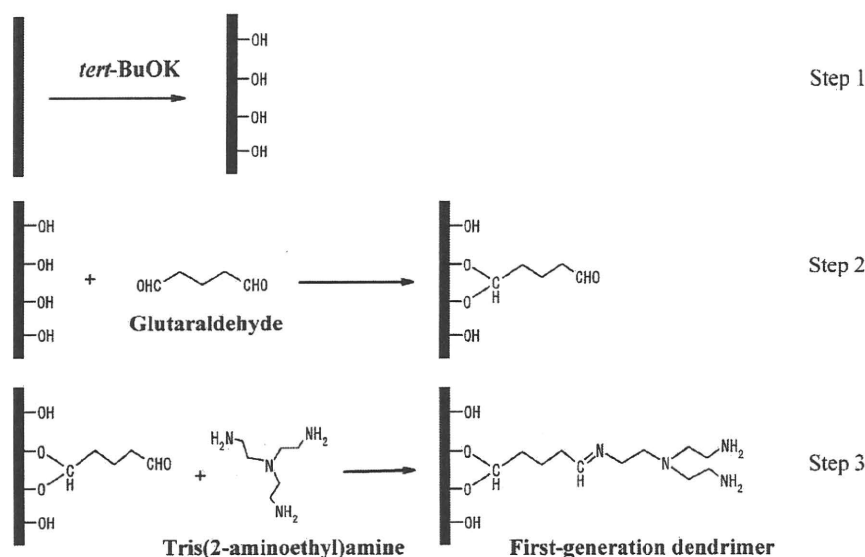
Fig. 2.  Schematic Illustration of Dendrimer Immobilization onto the Surface of Polystyrene Plate

肝細胞は，リガンドがフルクトース，ガラクトース単独のものに比べ，肝特異的機能であるウレア合成能が向上し，アルブミン遺伝子の発現も維持しており，機能維持についても優れていることが確認できた．また，共焦点レーザー顕微鏡による解析から，リガンドのないデンドリマー上のスフェロイド内部の細胞はアポトーシスを起こしているのに対し，F/Gデンドリマー上のスフェロイドではアポトーシスが抑制されていることを確認した．[7]

　リガンド修飾デンドリマーを基材表面上に固定し，細胞培養に用いるアイデアは筆者ら独自のものである．これまでの検討から，細胞毎に異なるリガンドを用いることで，リガンド修飾デンドリマーによって最適な細胞培養表面の創出が可能であることを示してきた．大阪大学基礎工学研究科の田谷正仁教授のグループは筆者らとの共同研究においてデンドリマーの密度を変化させることにより軟骨細胞の形態，分化機能を制御することに成功した．[8,9]またD-グルコースとEpidermal growth factorをリガンドとして用いると細胞の増殖及び運動性を亢進できることを報告している．[10]さらに大阪大学医学系研究科の宮崎純一教授のグループはD-グルコースをデンドリマーにより培養表面に提示するとES細胞の未分化能が有意に維持されることを見い出している．[11]このようにリガンド修飾デンドリマーは，細胞毎に最適化したカスタムメイドの培養基材表面創出のツールとなり，組織工学全般の発展に大きく貢献することが期待される．

**3.　3次元培養による肝機能制御**

　ラジアルフロー型バイオリアクター（RFB）は一般に円筒形のリアクター内に細胞接着用の担体を充填し円筒周囲より培養液あるいは血漿が中心部に向けて流れる構造をしている．RFBは従来のリアクターに比べ，潅流液の流速による剪断力が弱いため細胞障害が少なく，酸素や栄養物の供給がより均一に行われることが知られている．これまで動物細胞が $1 \times 10^8$ cells/ml 以上の高密度で培養可能であることが示されている．[12]筆者らはRFBをバイオ人工肝臓に応用することを目的とし多孔質ガラスビーズ（シランビーズ）を担体として肝細胞の潅流培養を行った．Figure 3にRFBを用いた培養システム図を示した．筆者らは骨髄間質細胞を肝細胞の生存性を延長し機能を強化するための支援細胞として選択した．骨髄間質細胞は骨髄においてコラーゲン，フィブロネクチンを始めとする細胞外マトリクスや種々の増殖因子を産生し，造血幹細胞や血球系の細胞の維持に重要な役割を演じていることが知られている．プラスティックディッシュによる2次元培養の実験より骨髄由来の間質細胞が肝細胞の機能を維持する効果があることを既に明らかにしており，[13]その効果が3次元担体を用いたRFBにおいて発現するか否かを検討した．

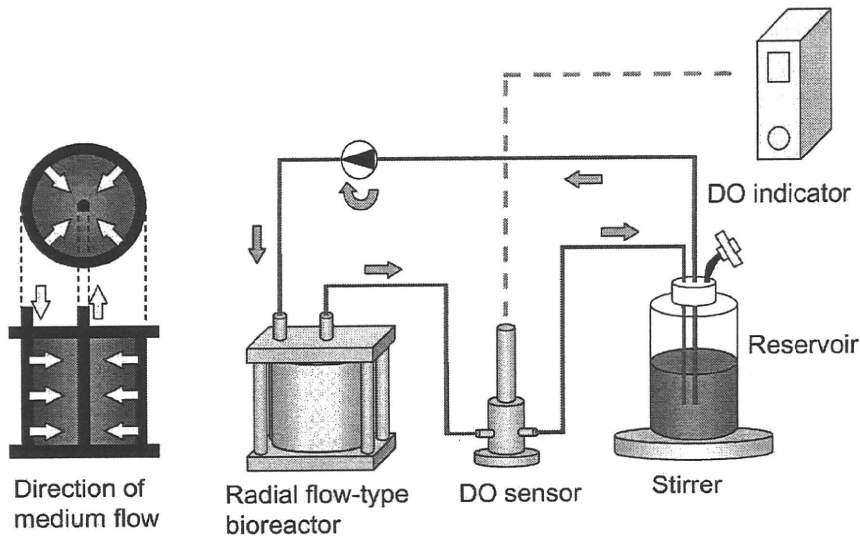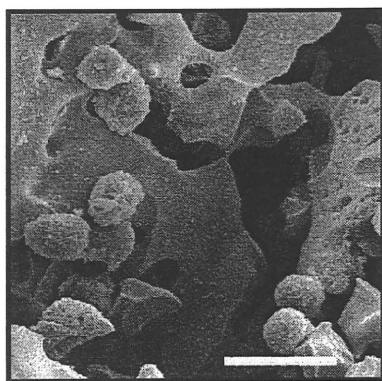　実験はSD系雄性ラット由来の細胞を用いて行った．肝細胞は生体内においては肝再生時旺盛に増殖

Fig. 3. Perfusion Culture of Hepatocytes by Radial Flow-type Bioreacor



**Hepatocyte monoculture**
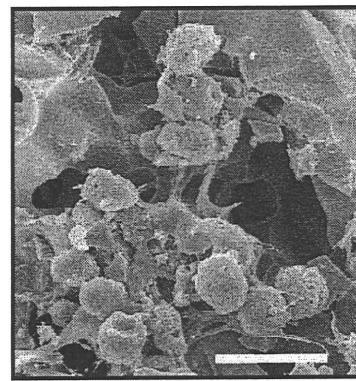
**Co-culture of hepatocytes and bone marrow stromal cells**

Fig. 4. Electron Micrographs of Hepatocytes Cultured in Silan Beads
White bar indicates 50 μm.

するが in vitro では増殖させることは困難であるため初期接着した細胞数を維持することが重要となる．一方骨髄間質細胞は in vitro で活発に増殖するため，共培養時には最初に骨髄間質細胞を播種し担体上でサブコンフルエントに達するまで培養した後に肝細胞を播種した．Figure 4 にシランビーズを用いた肝細胞単独培養，骨髄間質細胞との共培養を行った際の電子顕微鏡写真を示した．単独培養では直径約 15–20 ミクロンの球状をした肝細胞がシランビーズ上に接着している様子が観察される．一方共培養においてはシランビーズ上に伸展した骨髄間質細胞に肝細胞が接着していた．そしてそれぞれのシランビーズを充填した RFB を用いて 4 日間の連続

潅流培養を行った．その間 24 時間おきにサンプリングを行い，肝特異機能である尿素合成能を評価した．その結果，対照として行った肝細胞単独の 2 次元培養では 4 日間で機能は約 9％ に低下したが，RFB の 3 次元培養においては 29％ までの低下にとどまった．したがって RFB による潅流培養の効果が示された．さらに骨髄間質細胞との共培養により 47％ の機能が有意に維持され，肝細胞に対する効果が 2 次元培養のみならず RFB を用いた 3 次元培養においても発現することが明らかとなった．骨髄間質細胞は培養によって増幅することが可能でありヒト由来，あるいは患者自身の細胞を将来使用することも視野におくとバイオ人工肝臓の機能を強化し得

る細胞源として有望と考えている．さらには骨髄細胞中には肝細胞へ分化可能な間葉系幹細胞（MSC）が存在することから患者由来の細胞を利用した薬物代謝評価系の構築も可能であり個の医療への応用も期待される．

### 4. 遺伝子導入による肝機能制御

これまで肝がん細胞にアンモニア代謝，薬物代謝に係わる個々の遺伝子を導入する試みは国内の他グループにより報告されている．[14,15] われわれは人工肝臓が担うべき数百という肝機能を考慮し細胞全体をグローバルに活性化し，かつ細胞死に対する抵抗性を付与することを目的として遺伝子導入を試みている．

チオレドキシンと呼ばれるタンパク質はリボヌクレオチドリダクターゼの生理的還元剤として発見されたが酸化的ストレスやアポトーシスに対して抵抗性を付与するという機能が報告され注目を浴びている．[16,17] われわれはこのチオレドキシン遺伝子を肝細胞へ導入することにより生体外において引き起こされるストレス及びアポトーシスに対し抵抗性を獲得させることを試みた．肝細胞は生体外では増殖が困難であること，そして遺伝子導入効率を考慮しアデノウィルスをベクターとして用いることとした．ヒトチオレドキシン遺伝子を挿入した組換えアデノウィルスを作成しラット肝細胞へ感染させた．ヒトチオレドキシンが発現していることをウェスタンブロットで確認後，過酸化水素処理に対する抵抗性を調べた．1 mM 過酸化水素で 24 時間処理した後，アポトーシスを起こした細胞数を fluorescence activated cell sorting（FACS）により測定した．コントロールの肝細胞は約 80% がアポトーシスを起こしたのに対し，チオレドキシン遺伝子を導入した肝細胞は約 25% とアポトーシスに対して抵抗性を獲得したことが示された．また，通常のポリスチレンプレートで培養したときの寿命が延長されるか否かを調べたところ明らかな効果が観察された．尿素合成能も同時に維持されチオレドキシン遺伝子導入の有効性が示された．[18] リアクターへ充填する細胞へ当該遺伝子をウィルスベクターを用いて導入することも可能であり，またチオレドキシントランスジェニック動物を作出しその肝細胞をバイオ人工肝臓や医薬品開発のスクリーニング系に適用することも将来可能となるであろう．

### 5. 肝細胞源の検討

肝細胞源としてはヒトの細胞を用いることが理想的である．再生医療用の細胞源としてこれまで ES 細胞，骨髄細胞などが主に検討されてきたがわれわれは通常廃棄される組織から肝細胞へ分化可能な幹細胞を単離することができれば有用であると考えた．歯科領域では歯髄から MSC が単離されたことが報告されており，[19,20] 抜歯され廃棄される歯に着目した．虫歯の場合，病原菌が含まれ再生医療に適用することは困難であるため，歯科矯正時に抜歯される第 3 大臼歯，通称"親知らず"を用いることとした．矯正時に抜歯されるものは埋伏した状態であり，未分化な歯胚組織が維持されている可能性が高く，分化が進むと象牙質，歯髄となる歯乳頭組織には有用な MSC が存在することが予想された．そこでインフォームドコンセントを得た後，破棄された親知らずより歯乳頭組織を採取し MSC のクローン単離を試みた．

歯乳頭組織をはさみで細かく切断し，コラゲナーゼにより細胞を分散後組織培養用ディッシュに播種し α-MEM を用いて培養を行った．接着性の細胞を回収し FACS を用いて 96 穴プレートの 1 ウェルあたり 1 つの細胞が入るように播種した．単一細胞からコロニー形成したものを継代しさらに増殖させ，$2 \times 10^4$ cells を分化能の評価に使用し，残りの細胞を凍結保存した．カルセインを利用した骨分化能を指標として幹細胞としての特性を有するクローンの選択を行った結果，コロニー形成能を有するものの約 30% が骨分化能を発現した．その中から特に高い骨分化能を示したクローンを用いて以下の検討を行った．

肝細胞への分化誘導には Hamazaki らの方法[21]に準じ，HGF，デキサメタゾン，ITS に加えて線維芽細胞増殖因子（FGF），オンコスタチン M（OSM）を用いた．培養初期には細長い線維芽細胞用の形態であるが分化誘導を継続するにつれ，2 週間後にはサイズの大きい多角の形態へと変化した．RT-PCR による解析の結果，分化誘導 10 日でアルブミン遺伝子の発現が観察され，逆に初期分化マーカーである AFP 遺伝子発現は減少する傾向にあった．次に肝障害ラットを用いて移植の効果を検討した．

ヒト細胞を移植するため拒絶反応を起こさない免疫不全のヌードラットを使用した．9 週齢のフィッ

シャー344系ヌードラットの門脈から四塩化炭素
（1 ml/kg body weight）を週2回，4週間投与し肝
傷害を与えた．分化誘導培地あるいは非誘導培地で
培養後蛍光色素である PKH26 で染色し，四塩化炭
素初回投与2日後に門脈より $1 \times 10^7$ 個の細胞を移
植した．コントロールとしては四塩化炭素の替わり
にオリーブオイルを腹腔内投与したもの，及び四塩
化炭素を投与し細胞の替わりに生理食塩水を門脈か
ら投与したもの（sham operation）を用意した．凍
結肝臓切片を作成し蛍光観察を行った．細胞移植群
においては誘導培地，非誘導培地で培養した双方で
生着が確認された．骨髄由来の間葉系幹細胞
（BMSC）を移植した際には個々の蛍光が散在して
いたが，[22] 歯胚由来細胞移植の場合はコロニー状の
像が観察されたことから生着後に増殖したものと思
われる．In vitro の培養において歯胚由来細胞は
BMSC に比べ旺盛な増殖能を有しており，生着後
の増殖を可能にしたものと思われる．

　分化誘導した細胞の移植群では有意に血清 AST，
ALT 値の低下，肝線維化の抑制が観察された．非
誘導培地で培養した細胞を移植した群は肝臓内に生
着していたにもかかわらず有意な治癒効果は現われ
なかった．これらの結果より肝細胞への方向付けを
行うことが重要であることが示された．[23] このよう
に破棄される組織から再生医療に有用な幹細胞が得
られることは重要であり，自己の親知らずを抜歯し
た際，歯胚由来幹細胞を細胞バンクに保存しておけ
ば自身の細胞を肝疾患の治療に利用することが可能
となるであろう．また旺盛な増殖能があることから
移植までのつなぎとしてバイオ人工肝臓へ利用する
ことができること，医薬品スクリーニングの評価系
としても，倫理的な問題を持つ ES 細胞，強制的に
未分化状態に回帰させた iPS 細胞由来のものに比
べ有用であると考えている．

### 6. おわりに

　創薬の過程で毒性，有効性，及び薬物代謝の評価
に大量の動物が用いられてきたが，今後動物愛護の
観点から in vitro の評価に置き換えていくことが求
められている．肝細胞は毒性や薬物代謝を評価する
際に重要な役割を果たすことは明らかであるがこれ
まで初代培養細胞の不安定性から有用な評価系は構
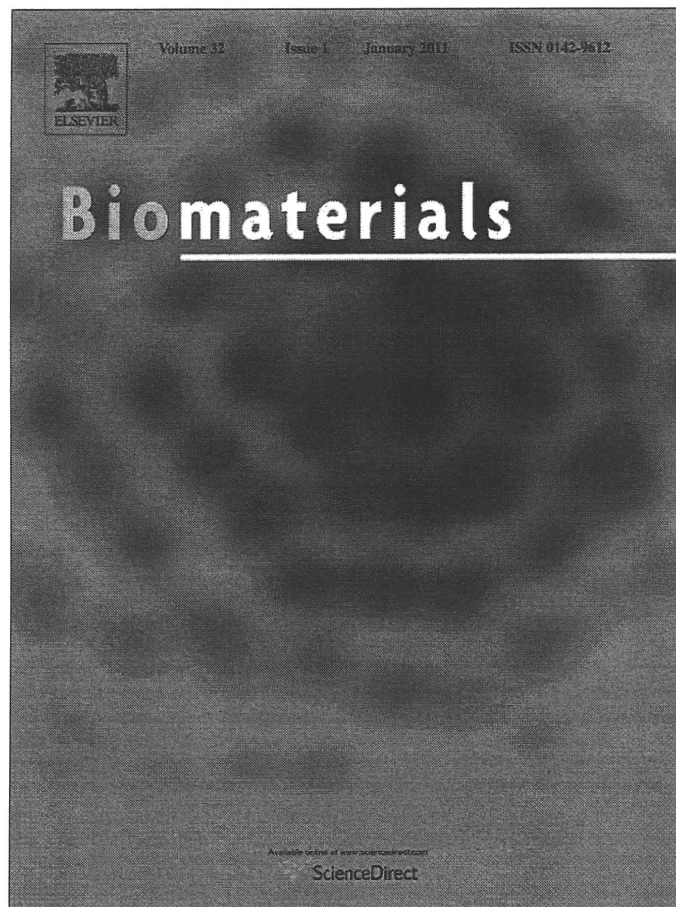築されていない．一般的に肝細胞のような足場依存
性の細胞は培養表面の性状によりその生存性，機能

が著しく変動することが知られている．本総説では
デンドリマーを用いる機能性培養基材の創製，3次
元培養による機能維持効果，また遺伝子導入による
寿命延長について筆者らの成果を紹介した．最小限
の細胞で評価系を構築することに役立つ技術開発に
つながればと願っている．さらに通常廃棄されるヒ
トの組織から肝細胞を分化誘導し細胞源として用い
ることができれば倫理的問題，種による差異を含め
種々の問題点を解決できることになろう．

## REFERENCES

1) Tomalia D. A., Baker H., Dewald J., Hall M.,
   Kallos G., Martin S., Roeck J., Ryder J.,
   Smith P., *Polym. J.*, **17**, 117–132 (1985).
2) Bielinska A., Kukowska-Latallo J. F., Joh-
   nson J., Tomalia D. A., Baker J. R. Jr.,
   *Nucleic Acids Res.*, **24**, 2176–2182 (1996).
3) Braun C. S., Vetro J. A., Tomalia D. A., Koe
   G. S., Koe J. G., Middaugh C. R., *J. Pharm.
   Sci.*, **94**, 423–436 (2005).
4) Svenson S., Tomalia D. A., *Adv. Drug Deliv.
   Rev.*, **57**, 2106–2129 (2005).
5) Tomalia D. A., Reyna L. A., Svenson S.,
   *Biochem. Soc. Trans.*, **35**, 61–67 (2007).
6) Kawase M., Shiomi T., Matsui H., Ouji Y.,
   Higashiyama S., Tsutsui T., Yagi K., *J.
   Biomed. Mater. Res.*, **54**, 519–524 (2001).
7) Higashiyama S., Noda M., Kawase M., Yagi
   K., *J. Biomed. Mater. Res.*, **64A**, 475–482
   (2003).
8) Kim M.-H., Kino-oka M., Kawase M., Yagi
   K., Taya M., *J. Biosci. Bioeng.*, **103**, 192–199
   (2007).
9) Kino-oka M., Morinaga Y., Kim M.-H.,
   Takezawa Y., Kawase M., Yagi K., Taya M.,
   *Biomaterials*, **28**, 1680–1688 (2007).
10) Kim M.-H., Kino-oka M., Kawase M., Yagi
    K., Taya M., *J. Biosci. Bioeng.*, **104**, 428–431
    (2007).
11) Mashayekhan S., Kim M.-H., Miyazaki S.,
    Tashiro F., Kino-oka M., Taya M., Miyazaki
    J.-I., *Biomaterials*, **29**, 4236–4243 (2008).
12) Hongo T., Kajikawa M., Ishida S., Ozawa S.,
    Ohno Y., Sawada J.-I., Umezawa A., Ishika-
    wa Y., Kobayashi T., Honda H., *J. Biosci.
    Bioeng.*, **99**, 237–244 (2005).
13) Isoda K., Takeda M., Higashiyama S., Ka-

wase M., Yagi K., *J. Biosci. Bioeng.*, **97**, 343–346 (2004).

14) Enosawa S., Miyashita T., Suzuki S., Li X. K., Tsunoda M., Amemiya H., Yamanaka M., Hiramatsu S., Tanimura N., Omasa T., Suga K., Matsumura T., *Cell Transplant.*, **9**, 711–715 (2000).

15) Wang N., Tsuruoka S., Yamamoto H., Enosawa S., Omasa T., Sata N., Matsumura T., Nagai H., Fujimura A., *Artif. Organs*, **29**, 681–684 (2005).

16) Saitoh M., Nishitoh H., Fujii M., Takeda K., Tobiume K., Sawada Y., Kawabata M., Miyazono K., Ichijo H., *EMBO J.*, **17**, 2596–2606 (1998).

17) Kondo N., Nakamura H., Masutani H., Yodoi J., *Antioxid. Redox Signal.*, **8**, 1881–1890 (2006).

18) Tsutsui T., Koide H., Fukahori H., Isoda K., Higashiyama S., Maeda I., Tashiro F., Yamato E., Miyazaki J., Yodoi J., Kawase M., Yagi K., *Biochem. Biophys. Res. Commun.*, **307**, 765–770 (2003).

19) Gronthos S., Mankani M., Brahim J., Robey P. G., Shi S., *Proc. Natl. Acad. Sci. USA*, **97**, 13625–13630 (2000).

20) Pierdomenico L., Bonsi L., Calvitti M., Rondelli D., Arpinati M., Chirumbolo G., Becchetti E., Marchionni C., Alviano F., Fossati V., Staffolani N., Franchina M., Grossi A., Bagnara G. P., *Transplantation*, **80**, 836–842 (2005).

21) Hamazaki T., Iiboshi Y., Oka M., Papst P. J., Meacham A. M., Zon L. I., Terada N., *FEBS Lett.*, **497**, 15–19 (2001).

22) Oyagi S., Hirose M., Kojima M., Okuyama M., Kawase M., Nakamura T., Ohgushi H., Yagi K., *J. Hepatol.*, **44**, 742–748 (2006).

23) Ikeda E., Yagi K., Kojima M., Yagyuu T., Ohshima A., Sobajima S., Tadokoro M., Katsube Y., Isoda K., Kondoh M., Kawase M., Go M., Adachi H., Yokota Y., Kirita T., Ohgushi H., *Differentiation*, **76**, 495–505 (2008).

# Development of an antibody proteomics system using a phage antibody library for efficient screening of biomarker proteins

Sunao Imai [a,1], Kazuya Nagano [a,1], Yasunobu Yoshida [a], Takayuki Okamura [a], Takuya Yamashita [a,b], Yasuhiro Abe [a], Tomoaki Yoshikawa [a,b], Yasuo Yoshioka [a,b,c], Haruhiko Kamada [a,c], Yohei Mukai [a,b], Shinsaku Nakagawa [b,c], Yasuo Tsutsumi [a,b,c], Shin-ichi Tsunoda [a,b,c,*]

[a] Laboratory of Biopharmaceutical Research, National Institute of Biomedical Innovation, 7-6-8 Saito-Asagi, Ibaraki, Osaka 567-0085, Japan
[b] Graduate School of Pharmaceutical Sciences, Osaka University, 1-6 Yamadaoka, Suita, Osaka 565-0871, Japan
[c] The Center of Advanced Medical Engineering and informatics, Osaka University, 1-6 Yamadaoka, Suita, Osaka 565-0871, Japan

## ARTICLE INFO

## ABSTRACT

Proteomics-based analysis is currently the most promising approach for identifying biomarker proteins for use in drug development. However, many candidate biomarker proteins that are over- or under-expressed in diseased tissues are found by such a procedure. Thus, establishment of an efficient method for screening and validating the more valuable targets is urgently required. Here, we describe the development of an "antibody proteomics system" that facilitates the screening of biomarker proteins from many candidates by rapid preparation of cross-reacting antibodies using phage antibody library technology. Using two-dimensional differential in-gel electrophoresis analysis, 16 over-expressed proteins from breast cancer cells were identified. Specifically, proteins were recovered from the gel pieces and a portion of each sample was used for mass spectrometry analysis. The remainder was immobilized onto a nitrocellulose membrane for antibody-expressing phage enrichment and selection. Using this procedure, antibody-expressing phages against each protein were successfully isolated within two weeks. The expression profiles of the identified proteins were then acquired by immunostaining of breast tumor tissue microarrays with the antibody-expressing phages. Using this approach, expression of Eph receptor A10, TRAIL-R2 and Cytokeratin 8 in breast tumor tissues were successfully validated.

These results demonstrate the antibody proteomics system is an efficient method for screening tumor-related biomarker proteins.

## 1. Introduction

Proteomics-based analysis is the most promising approach for identifying tumor-related biomarker proteins used in the drug development process [1–3]. The technological development of proteomics to seek and identify differentially expressed proteins in disease samples is expanding rapidly. However, in spite of the identification of many candidate biomarkers, the number of biomarker proteins successfully applied to drug development has been limited. The main difficulty is the lack of a methodology to comprehensively analyze the expression or function of many candidate proteins and to efficiently select potential biomarker proteins of interest. To circumvent this problem, an improved technology to efficiently screen the truly valuable proteins from a large number of candidates is desirable.

Monoclonal antibodies are extremely useful tools for the functional and distributional analysis of proteins [4–6]. For example, they can be applied to the specific detection and study of proteins through various techniques including ELISA, Western blotting, fluorescent imaging and tissue microarray analysis (TMA). Of all these techniques, TMA is particularly valuable because it enables the analysis of clinical expression profiles of antigens from many clinical samples [7–11]. However, the common hybridoma-based antibody production is a laborious and time-consuming method. Thus, it is impractical to create antibodies against many differentially expressed proteins identified by proteomics technologies, such as two-dimensional differential in-gel electrophoresis (2D-DIGE) [12–15]. Furthermore, a relatively large amount of antigen (several milligrams) is necessary to produce an antibody (i.e., immunization of animals or screening of positive clones). The

production of protein on this scale often requires engineering the corresponding gene for heterologous expression, which may require some time to optimize. In this respect, phage antibody library technology is able to construct a large repertoire protein or peptide consisting of hundreds of millions of molecules. Monoclonal antibodies against target antigens are then rapidly obtained from the phage libraries displaying single chain fragment variable (scFv) antibodies *in vitro* [16–21].

However, the amount of protein in spots detected by 2D-DIGE analysis is generally very small (hundreds of nanograms). Therefore, a technology for generating monoclonal antibodies from such small amounts of antigen needs to be developed. There are no reports that describe the successful isolation of antibodies against small amounts of proteins obtained from differential proteome analysis.

Here, we report the establishment of a method for the efficient isolation of scFv antibody-expressing phages from a small amount of protein antigen prepared *via* 2D-DIGE spots using a high quality non-immune mouse scFv phage library [22]. We also describe an efficient method for screening and validating tumor-related biomarker proteins of interest from a number of differentially expressed proteins by expression profiling using TMA and scFv antibody-expressing phages.

## 2. Materials and methods

### 2.1. Non-immune mouse scFv phage library

Construction of the improved non-immune murine scFv phage library has been described previously [22]. The phage library was prepared from a TG1 glycerol stock containing the scFv gene library.

### 2.2. Affinity panning using BIAcore® and nitrocellulose membrane

Three different amounts (5000 ng, 50 ng or 0.5 ng) of KDR-Fc chimera (R&D systems Inc., Minneapolis, MN) or a portion of the proteins (1–5 ng) extracted from 2D-DIGE spots were immobilized on a BIAcore sensor chip CM3® (BIAcore, Uppsala, Sweden) or on a nitrocellulose membrane. BIAcore-based panning has been described previously [22]. Membrane-based panning was performed using the Bio-Dot Microfiltration Apparatus (Bio-Rad Laboratories, Hercules, CA). The membrane was incubated with blocking solution (10% skimmed milk, 25% glycerol) for 2 h and then washed twice with 0.1% TBST (Tris-buffered saline containing 0.1% Tween 20). The model phage library (anti-KDR scFv antibody-expressing phages: wild type phage = 1: 100) or the non-immune scFv phage library was pre-incubated with 90% blocking solution at 4 °C for 1 h and then applied to each well. After 2–3 h incubation, the apparatus was washed ten times with TBST. Bound scFv antibody-expressing phages were then eluted with 100 mM triethylamine. The eluted phages were incubated in log phase E. coli TG1 cells and glycerol-stocks prepared for further repeat panning cycles. Phage titer was measured by counting the number of infected colony cells on Petrifilm (3M Co., St. Paul, MN).

### 2.3. Colony direct PCR

After the panning, colonies of phage-infected TG1 were picked up at random as PCR templates. The gene inserts of 16 clones were amplified by PCR using the following primers: primer-156 (5′-CAACGTGAAAAAATTATTATTCGC-3′) and primer-158 (5′-GTAAATGA ATTTTCTGTATGAGG-3′), which anneal to the sequences of pCANTAB5E phagemid vector (GE Healthcare Biosciences AB, Uppsala, Sweden). The size of insert DNA sequence was analyzed by agarose gel electrophoresis.

### 2.4. Cell lines

Human mammary gland cell line 184A1 (American Type Culture Collection; ATCC, Manassas, VA) was maintained by MEGM Bullet Kit (Takara Bio, Shiga, JAPAN). Mammary gland-derived breast cancer cell line SKBR3 (ATCC) was maintained in McCoy's 5a plus 10% FBS. All cells were grown at 37 °C in a humidified incubator with 5% $CO_2$.

### 2.5. 2D-DIGE analysis

Cell lysates were prepared from human mammary gland cell line 184A1 and mammary gland-derived breast cancer cell line SKBR3, and then solubilized with 7 M urea, 2 M thiourea, 4% CHAPS and 10 mM Tris–HCl (pH 8.5). The lysates were labeled at the ratio 50 µg protein: 400 pmol Cy3 or Cy5 protein labeling dye (GE Healthcare

Biosciences AB) in dimethylformamide according to the manufacture's protocol. For first dimension separation, the labeled samples (each 50 µg) were combined and mixed with rehydration buffer (7 M urea, 2 M thiourea, 4% CHAPS, 2% DTT, 2% Pharmalyte (GE Healthcare Biosciences AB)) and applied to a 24-cm immobilized pH gradient gel strip (IPG-strip pH 5–6 NL). The samples for the spot-picking gel were prepared without labelling by Cy-dyes. For the second dimension separation, the IPG-strips were applied to SDS-PAGE gels (10% polyacrylamide and 2.7% N,N′-diallyltartardiamide gels). After electrophoresis, the gels were scanned with a laser fluoroimager (Typhoon Trio, GE Healthcare Biosciences AB). The spot-picking gel was scanned after staining with Flamingo solution (Bio-Rad). Quantitative analysis of protein spots was carried out with Decyder-DIA software (GE Healthcare Biosciences AB). For the antigen spots of interest, spots of 1 × 1 mm in size were picked using an Ettan Spot Picker (GE Healthcare Biosciences AB). Proteins were extracted by solubilizing the picked gel pieces using 88 mM sodium periodide. Protein volumes were determined by BSA standard in Colloid Gold Total Protein staining (Bio-Rad).

### 2.6. In-gel tryptic digestion

Spots of 1 mm × 1 mm in size were picked using an Ettan Spot Picker and digested with trypsin as described below. The gel pieces were then destained with 50% acetonitrile/50 mM NH4HCO3 for 20 min twice, dehydrated with 75% acetonitrile for 20 min, and then dried using a centrifugal concentrator. Next, 5 µl of 20 µl/ml trypsin (Promega, Madison, WI) solution was added to each gel piece and incubated for 16 h at 37 °C. Three solutions were used to extract the resulting peptide mixtures from the gel pieces. First, 50 µl of 50% (v/v) acetonitrile in 1% (v/v) aqueous trifluoroacetic acid (TFA) was added to the gel pieces, which were then sonicated for 5 min. Next, we collected the solution and added 80% (v/v) acetonitrile in 0.2% TFA. Finally, 100% acetonitrile was added for the last extraction. The peptides were dried and then resuspended in 10 µl of 0.1% TFA before being cleaned using ZipTip™ µC18 pipette tips (Millipore, Billerica, MA). The tips were wetted with three washes in 50% acetonitrile and equilibrated with three washes in 0.1% TFA, then the peptides were aspirated 10 times to ensure binding to the column. The column and peptides were washed three times in 0.1% TFA before being eluted in 1 µl of 80% acetonitrile/0.2% TFA.

### 2.7. Mass spectrometry (MS) and database search

The tryptic digests (0.6 µl) were mixed with 0.6 µl α-cyano-4-hydroxy-transcinnamic acid saturated in a 0.1% TFA and acetonitrile solution (1:1vol/vol). Each mixture was deposited onto a well of a 96-well target plate and then analyzed by matrix-assisted laser desorption ionization time-of-flight mass spectrometry (MALDI-TOF/MS; autoflexII, Bruker Daltonics, Billerica, WI) in the Reflectron mode. The mass axis was adjusted with calibration peptide (BRUKER DALTNICS) peaks (M/z 1047.19, 1296.68, or 2465.19) as lock masses. Bioinformatic databases were searched to identify the proteins based on the tryptic fragment sizes. The Mascot search engine (http://www.matrixscience.com) was initially used to query the entire theoretical tryptic peptide as well as SwissProt (http://www.expasy.org/, a public domain database provided by the Swiss Institute of Bioinformatics, Geneva, Switzerland). The search query assumed the following: (i) the peptides were monoisotopic (ii) methionine residues may be oxidized (iii) all cysteines are modified with iodoacetamide.

### 2.8. Phage ELISA using nitrocellulose membrane

Phage ELISA using scFv antibody-expressing phages was performed as previously described [22]. Briefly, phage-infected TG1 clones were picked, monocloned in a Bio-Dot Microfiltration Apparatus and scFv antibody-expressing phages propagated. The supernatants containing scFv antibody-expressing phages were incubated with immobilized proteins (~1 ng) extracted from 2D-DIGE spots. scFv antibody-expressing phages bound to 2D-DIGE spots were visualized using HRP-conjugated anti-M13 monoclonal antibody (GE Healthcare Biosciences AB).

### 2.9. Immunohistochemical staining using scFv antibody-expressing phages

Human breast cancer and normal TMA (Super Bio Chips, Seoul, South Korea & Biomax, Rockville, MD) were deparaffinated in xylene and rehydrated in a graded series of ethanol. Heat-induced epitope retrieval was performed in while keeping Target Retrieval Solution pH 9 (Dako, Glostrup, Denmark) temperature following the manufacturer's instructions. Heat-induced epitope retrieval was performed while maintaining the Target Retrieval Solution pH 9 (Dako) at the desired temperature according to the manufacturer's instructions. After heat-induced epitope retrieval treatment, endogenous peroxidase was blocked with 0.3% $H_2O_2$ in TBS for 5 min followed by washing twice in TBS. TMA were incubated with 5% BSA blocking solution for 15 min. The slides were then incubated with the primary scFv antibody-expressing phages ($10^{12}$ CFU/ml) for 60 min. After washing three times with 0.05% TBST, each series of sections was incubated for 30 min with ENVISION + Dual Link (Dako), washed three times in TBST. The reaction products were rinsed twice with TBST, and then developed in liquid 3,3′-diaminobenzidine (Dako) for 3 min. After the development, sections were washed twice with distilled water, lightly

counterstained with Mayer's hematoxylin, dehydrated, cleared, and mounted with resinous mounting medium. All procedures were performed using AutoStainer (Dako).

### 2.10. TMA immunohistochemistry scoring

The optimized staining condition for breast tumor tissue microarray was determined based on the coexistence of both positive and negative cells in the same tissue sample. Signals were considered positive when reaction products were localized in the expected cellular component. The criteria for the staining were scored as follows: distribution score was scored as 0 (0%), 1 (1–50%), and 2 (51–100%) to indicate the percentage of positive cells in all tumor cells present in one tissue. The intensity of the signal (intensity score) was scored as 0 (no signal), 1 (weak), 2 (moderate) or 3 (marked). The total of the distribution score and intensity score was then summed into a total score (TS) of TS0 (sum = 0), TS1 (sum = 2), TS2 (sum = 3), and TS3 (sum = 4–5). Throughout this study, TS0 or TS1 was regarded as negative, whereas TS2 or TS3 was regarded as positive. Statview software was used in statistical analysis.

## 3. Results

### 3.1. Optimization of panning methods

To establish a method for the efficient isolation of antibodies against a small amount of protein antigen (nanogram-order or less) prepared from 2D-DIGE spots, 5000 ng, 50 ng or 0.5 ng of recombinant KDR proteins were first immobilized on a BIAcore sensor chip CM3® or on a nitrocellulose membrane using the Bio-Dot Microfiltration Apparatus®. Isolation of antibodies was assessed using a model phage library (anti-KDR scFv antibody-expressing phages: wild type phage = 1: 100) (Fig. 1). Enrichment of the desired clones in the output library was evaluated by analyzing the gene inserts of randomly-picked phage-infected TG1 cells by colony direct PCR. In the method using BIAcore®, enrichment was observed when 5000 ng of KDR was used for immobilization. By contrast, Membrane-based panning led to the successful enrichment of anti-KDR scFv antibodies from only 0.5 ng of KDR. These results demonstrated that membrane-based panning was suitable for the isolation of antibodies from very small amounts of antigen extracted from 2D-DIGE spot gel pieces.

### 3.2. 2D-DIGE analysis and identification of differentially expressed proteins

To identify breast tumor-related biomarker proteins and isolate monoclonal antibodies against them, we performed 2D-DIGE using breast cancer cell lines SKBR3 and normal breast cell lines 184A1 (Fig. 2). Quantitative analysis showed that 21 spots displayed increased or decreased expression levels in the cancer cell line compared with the normal cell line. MALDI-TOF/MS analysis of the spots subsequently identified 16 different proteins (Table 1).

### 3.3. Isolation of antibodies against each 2D-DIGE spot from the non-immune scFv phage library

The amount of protein extracted from the gel pieces ranged from several tens of nanogram to a few micrograms (Table 1). Because the membrane-based panning method facilitates the isolation of antibodies from 0.5 ng of protein (Fig. 1), we reasoned that this method could be used to isolate antibodies from the small amounts of proteins extracted from 2D-DIGE spot gel pieces. Thus a portion of the extracted proteins were immobilized onto nitrocellulose membranes by means of a Bio-Dot Microfiltration Apparatus, and membrane-based panning was performed using the non-immune scFv phage library [22] (Table 2). The results from this panning showed that the output/input ratio of phage titer (titer of the recovered phage library after the panning/titer of phage library before the panning) after the fourth round of panning against all spots increased approximately 20-fold–4000-fold in comparison to that obtained from the first round of panning. This elevated output/input ratio indicated the enrichment of the antigen-binding scFv antibody clones. To isolate monoclonal scFv antibodies to each spot, a total of 60 clones were randomly picked from the 4th panning output phage library and binding of the monoclonal scFv antibody-expressing phages to each antigen was tested by phage ELISA. As a result, several scFv antibody clones binding to each of the 16 antigens were isolated (Table 2). The antigenic specificity of isolated scFv antibodies was investigated by dot blot using various proteins as antigens. Some of the isolated scFv antibodies bound specifically to the antigen protein, but not to the His-tagged caspase-8, His-tagged importin-β, tumor necrosis factor receptor 1 (TNFR1)-Fc-chimera and KDR-Fc-chimera (data not shown). These results indicated the successful isolation of each spot-specific scFv antibody-expressing phages after only two weeks.

### 3.4. TMA analysis

The next stage in the process was to select the most valuable breast tumor-related biomarker proteins from a large number of
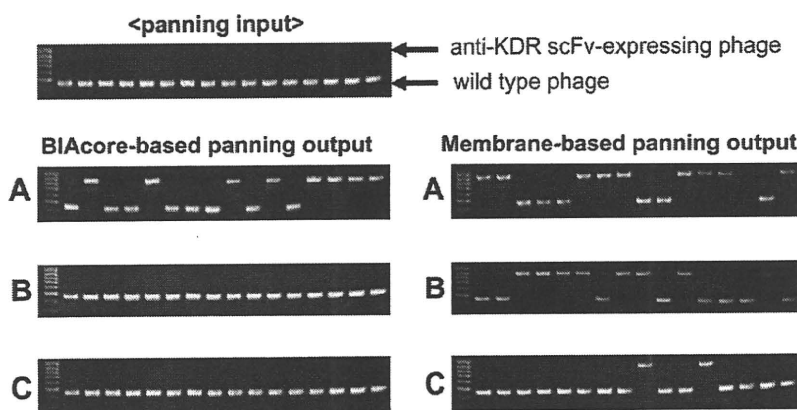


**Fig. 1.** Optimization of panning methods to isolate monoclonal antibodies from a very small amount of antigen. Model panning was performed using the BIAcore® or nitrocellulose membrane. The model library (anti-KDR scFv phage : wild type phage = 1: 100) was incubated with KDR ((A) 5000 ng, (B) 50 ng, (C) 0.5 ng) immobilized on a sensor chip or nitrocellulose membrane. The BIAcore-based panning method has been previously described [22]. After the binding step, the nitrocellulose membrane was washed ten times with TBST. The bound scFv antibody-expressing phages were eluted with triethylamine. The eluted scFv antibody-expressing phages were then incubated in log phase TG1 cells and individual TG1 clones were picked at random. Inserts of 16 phage clones were amplified by PCR. The gene sizes of inserts were analyzed by agarose gel electrophoresis.
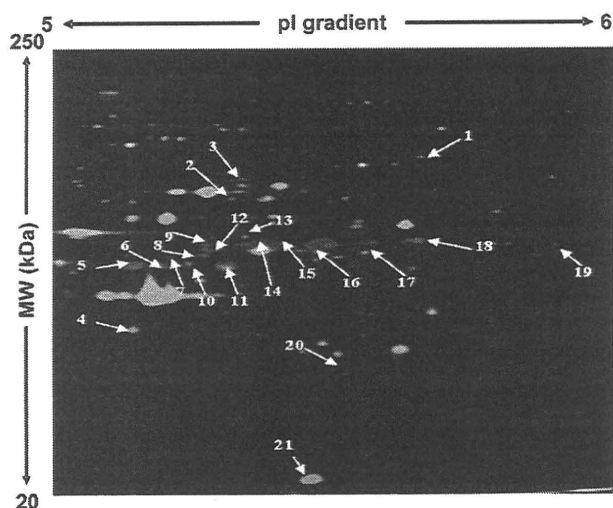
**Fig. 2.** 2D-DIGE image of fluorescently labeled proteins from SKBR3 and 184A cell. Breast cancer cell line (SKBR3) and normal breast cell line (184A1) were labeled using cy3 and cy5, respectively. The protein samples were then subjected to 2D electrophoresis. Spots that were over- and under-expressed in mammary cancer cells relative to normal cells were colored red and green, respectively. Yellow color spots show no change in expression.

**Table 2**
Enrichment and isolation of antibodies to 2D-DIGE spots from non-immune libraries.

| Spot | Protein name | Output/Input Ratio ($\times 10^{-7}$)/round | | | | The number of isolated mAb. |
|------|--------------|------|-----|-----|-----|------|
| | | 1st | 2nd | 3rd | 4th | |
| #1 | splicing factor YT521-B | 6 | 7 | 16 | 480 | 4 |
| #2 | IkappaBR | 6 | 7 | 15 | 500 | 3 |
| #3 | SPATA5 | 5 | 6 | 32 | 860 | 2 |
| #4 | skin aspartic protease | 5 | 6 | 5 | 24 | 1 |
| #5 | beta actin variant | 7 | 11 | 17 | 480 | 1 |
| #6 | TRAIL-R2 | 6 | 7 | 25 | 420 | 5 |
| #7 | Cytokeratin 18 | 5 | 11 | 62 | 260 | 4 |
| #8 | TRAIL-R2 | 5 | 27 | 41 | 1500 | 5 |
| #9 | RREB1 | 8 | 9 | 14 | 370 | 7 |
| #10 | Cytokeratin 7 | 6 | 7 | 3 | 2200 | 5 |
| #11 | Cytokeratin 18 | 6 | 8 | 15 | 84 | 2 |
| #12 | Cytokeratin 7 | 10 | 11 | 13 | 94 | 2 |
| #13 | FLJ31438 | 7 | 9 | 32 | 80 | 6 |
| #14 | Cytokeratin 7 | 4 | 7 | 46 | 280 | 5 |
| #15 | PAK65 | 7 | 11 | 51 | 580 | 9 |
| #16 | Cytokeratin 8 | 8 | 7 | 16 | 4100 | 6 |
| #17 | Cytokeratin 8 | 5 | 12 | 33 | 240 | 2 |
| #18 | XRN1 | 6 | 20 | 18 | 200 | 1 |
| #19 | Jerky protein homolog-like | 7 | 10 | 49 | 940 | 3 |
| #20 | Eph receptor A10 | 8 | 6 | 57 | 3000 | 2 |
| #21 | Glutathione S-transferase P | 7 | 8 | 110 | 1900 | 2 |

identified candidate proteins. To this end, we immunostained TMA slides with 189 cases of breast tumors and 15 cases of normal breast specimens using the isolated spot-specific scFv antibody-expressing phages and screened the promising candidate biomarker proteins in terms of the expression profile in breast tumor tissues and normal tissues (Table 3). The result of the expression profile analysis showed that SPATA5, beta-actin variant, FLJ31438, PAK65, XRN1 and Jerky protein homolog-like were not expressed in

normal and breast cancer tissue at all. By contrast, TRAIL-R2, Cytokeratin 8 and Eph receptor A10 were highly and specifically expressed (Fig. 3) in 63, 73 and 49% of breast tumor cases respectively, while the existing-breast cancer marker, Her-2, was expressed in 28% of breast tumor cases (Table 3). Thus, the relationship between the expression of each antigen and the Her-2 expression profile was analyzed. The level of expression of TRAIL-R2, Cytokeratin 8 and Eph receptor A10 in Her-2 positive cases were 77, 77 and 62%, and in Her-2 negative cases were 57, 67 and 44%, respectively (Table 4). Furthermore, the relationship between the expression of each antigen and clinical stage was analyzed in 187 of the 189 cases where all the clinical data was available. The level of expression of Cytokeratin 8 and Eph receptor A10 increased with progression of clinical symptoms (Table 5).

## 4. Discussion

Here, we aimed to develop a method of efficiently screening tumor-related biomarker proteins by proteome analysis. In

**Table 1**
Identification of 2D-DIGE spots by MALDI-TOF/MS.

| Spot | Protein name | Accession number | MW (kDa) | pI | Protein volume (ng) | Expression ratio [cancer/ normal] (fold) |
|------|--------------|------------------|----------|-----|---------------------|------------------------------------------|
| #1 | splicing factor YT521-B | Q96MU7 | 85 | 5.9 | 119 | 6 |
| #2 | IkappaBR | Q96HA7 | 63 | 5.5 | 104 | 6 |
| #3 | SPATA5 | C9JT97 | 76 | 5.6 | 94 | 7 |
| #4 | skin aspartic protease | Q53RT3 | 37 | 5.3 | 610 | 0.1 |
| #5 | beta actin variant | P60709 | 42 | 5.3 | 99 | 15 |
| #6 | TRAIL-R2 | O14763 | 48 | 5.4 | 100 | 18 |
| #7 | Cytokeratin-18 | P05783 | 48 | 5.3 | 99 | 12 |
| #8 | TRAIL-R2 | O14763 | 48 | 5.4 | 95 | 16 |
| #9 | RREB1 | Q92766 | 52 | 5.3 | 109 | 10 |
| #10 | Cytokeratin-7 | P08729 | 51 | 5.4 | 126 | 23 |
| #11 | Cytokeratin-18 | P05783 | 48 | 5.3 | 497 | 13 |
| #12 | Cytokeratin-7 | P08729 | 51 | 5.4 | 122 | 24 |
| #13 | FLJ31438 | Q96N41 | 53 | 5.5 | 126 | 35 |
| #14 | Cytokeratin-7 | P08729 | 51 | 5.4 | 406 | 36 |
| #15 | PAK65 | Q13177 | 55 | 5.7 | 677 | 8 |
| #16 | Cytokeratin 8 | P05787 | 54 | 5.5 | 694 | 32 |
| #17 | Cytokeratin 8 | P05787 | 54 | 5.5 | 1143 | 72 |
| #18 | XRN1 | Q8IZH2 | 54 | 5.8 | 353 | 8 |
| #19 | Jerky protein homolog-like | Q9Y4A0 | 51 | 6.0 | 130 | 22 |
| #20 | Eph receptor A10 | Q5JZY3 | 32 | 5.7 | 119 | 9 |
| #21 | Glutathione S-transferase P | P09211 | 23 | 5.4 | 119 | 0.02 |

**Table 3**
Positive rate of identified proteins in breast cancer and normal breast tissues.

| Protein name | Positive rate of antigens | | | |
|--------------|---------------------------|---|-----------------------|---|
| | Normal breast tissues | | Breast cancer tissues | |
| Her-2 | 0/15 | (0%) | 53/189 | (28%) |
| IkappaBR | 3/15 | (20%) | 22/189 | (12%) |
| SPATA5 | 0/15 | (0%) | 0/189 | (0%) |
| beta actin variant | 0/15 | (0%) | 0/189 | (0%) |
| TRAIL-R2 | 0/15 | (0%) | 119/189 | (63%) |
| RREB1 | 1/15 | (7%) | 83/189 | (44%) |
| FLJ31438 | 0/15 | (0%) | 0/189 | (0%) |
| PAK65 | 0/15 | (0%) | 0/189 | (0%) |
| Cytokeratin 8 | 0/15 | (0%) | 137/189 | (73%) |
| XRN1 | 0/15 | (0%) | 0/189 | (0%) |
| Jerky protein homolog-like | 0/15 | (0%) | 0/189 | (0%) |
| Eph receptor A10 | 0/15 | (0%) | 93/189 | (49%) |

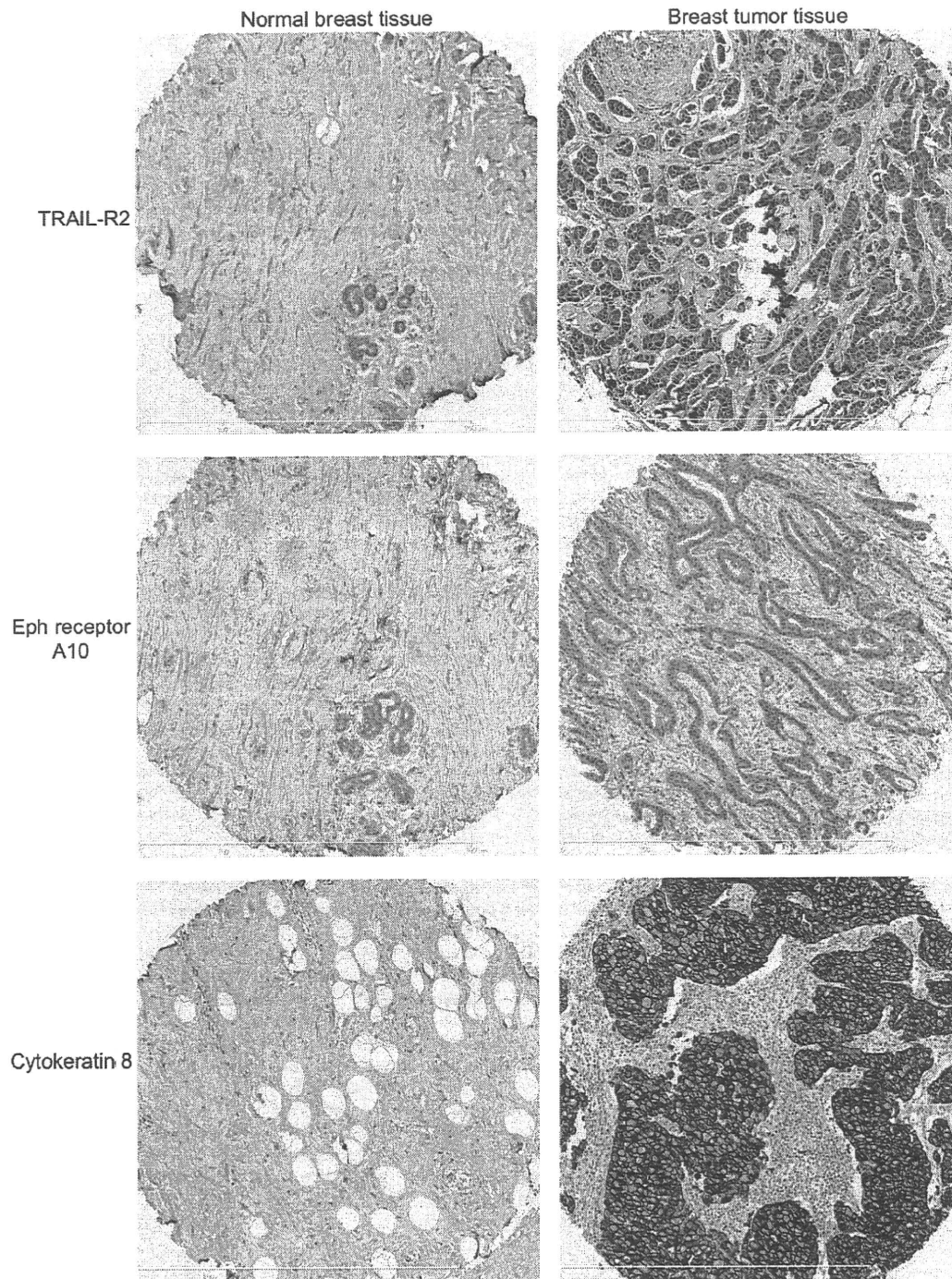| Normal breast tissue | Breast tumor tissue |
|---|---|



**Fig. 3.** Immunohistochemical staining of breast tumor and normal breast tissue microarray by scFv antibody-expressing phages. Typical images of breast cancer and normal breast tissue microarray stained by using scFv antibody-expressing phages to TRAIL-R2, Eph receptor A10 and Cytokeratin 8 are shown. Left panels are normal breast tissues and right panels are breast tumors. The tissue microarrays were counterstained by hematoxylin.

particular, we attempted to establish a means of isolating specific antibodies directly from small amounts of differentially expressed proteins obtained *via* 2D-DIGE analysis. To achieve this, we focused on a non-immune scFv phage library. Because the non-immune naïve scFv phage library has a huge repertoire of scFv on the surface of the phages, monoclonal antibodies to every antigen could be effectively isolated *in vitro*. Generally the diversity of the CDR3 domain, which is important for antigen-binding specificity, is

estimated to be approximately twenty million [23]. Thus we reasoned that our previously constructed library, containing $2.4 \times 10^9$ scFv variants, has almost equal potential as the murine or human immune system [22]. Initially, in order to isolate monoclonal antibodies against very small amounts of antigen (hundreds of nanograms) recovered from the spots of 2D-DIGE analysis, we attempted to optimize the panning method using either a BIAcore® or nitrocellulose membrane. In the method using BIAcore®, the

**Table 4**
Positive rate of identified proteins in Her-2 positive and Her-2 negative cases.

| Protein name | Positive rate of antigens in Her-2 | |
|---|---|---|
| | Positive cases | Negative cases |
| TRAIL-R2 | 41/53 (77%) | 78/136 (57%) |
| Cytokeratin 8 | 41/53 (77%) | 91/136 (67%) |
| Eph receptor A10 | 33/53 (62%) | 60/136 (44%) |
| TRAIL-R2 or Eph receptor A10 | 46/53 (87%) | 100/136 (74%) |

**Table 5**
Positive rate of identified proteins in clinical stage.

| Protein name | Positive rate of antigens in clinical stage | | | | | |
|---|---|---|---|---|---|---|
| | Stage I | | Stage II | | Stage III | |
| Her-2 | 6/14 | (43%) | 17/87 | (20%) | 30/86 | (35%) |
| TRAIL-R2 | 11/14 | (79%) | 51/87 | (59%) | 55/86 | (64%) |
| Cytokeratin 8* | 7/14 | (50%) | 58/87 | (67%) | 71/86 | (83%) |
| Eph receptor A10* | 4/14 | (29%) | 42/87 | (48%) | 47/86 | (55%) |

Man Whitney $U$ test *$P < 0.05$

enrichment of the desired clones was observed when immobilizing 5000 ng of KDR. By contrast, membrane-based panning led to the successful enrichment of clones from only 0.5 ng of KDR (Fig. 1). BIAcore-based panning has been recognized to be an effective method because the interaction of an antigen and a scFv antibody can be monitored in real time and the operation can be automated [24,25]. However, our results suggest that BIAcore® is inefficient for immobilizing very small amounts of antigen. This is because antigen immobilization using the BIAcore procedure requires a chemical coupling reaction with the surface of the sensor chip. In contrast, the membrane-based panning method is suitable for the isolation of antibodies against very small amounts of antigens. The suitability of this procedure when handling such small amounts of proteins presumably arises from the high efficiency of adsorption of antigens by the nitrocellulose membrane. These results show that monoclonal antibodies can be created from small amounts of proteins recovered from 2D-DIGE spots.

In breast cancer patients, the antibody targeting human epidermal growth factor receptor II (Her-2), is an effective drug [26,27]. However, because this receptor is over-expressed in only ~25% of breast cancer patients, anti-Her-2 antibody therapy is ineffective in ~75% of cases. Furthemore, approximately 30% of Her-2 over-expressed patients that received anti-Her-2 antibody therapy became tolerant [28–30]. Thus, we applied our antibody

proteomics system to breast cancer samples for identification of the proteins to replace Her-2 as suitable therapeutic targets. Initially, 21 differentially expressed proteins between SKBR3 and 184A1 cells were found by 2D-DIGE analysis and 16 different proteins were identified by MALDI-TOF/MS. Four of the identified proteins were present in more than one spot i.e., TRAIL-R2 (spot 6, 8), Cytokeratin 18 (spot 7, 11), Cytokeratin 8 (spot 16, 17) and Cytokeratin 7 (spot 10, 12, 14). These proteins presumably display different pI and MW values due to posttranslational modification. Next, membrane-based panning against these spots was performed, and the output/input ratio of phage titer after the fourth round of panning increased from approximately 20-fold–4000-fold in comparison to that after the first round of panning. Moreover, we screened scFv antibody-expressing phages binding to each spot protein by phage ELISA and obtained each spot-specific scFv antibodies from all spots after approximately two weeks. Finally, it was necessary to select the most valuable proteins from a large number of differentially expressed proteins in breast cancer cells. Using the isolated spot-specific scFv antibody-expressing phages, we immunostained a TMA with 189 cases of breast cancer tissue and 15 samples of normal tissue. SPATA5, Beta actin, FLJ31438, PAK65 and XRN1 were not detected in either the tumor tissue or normal tissue. Thus, these proteins may have been derived from cell lines used in the
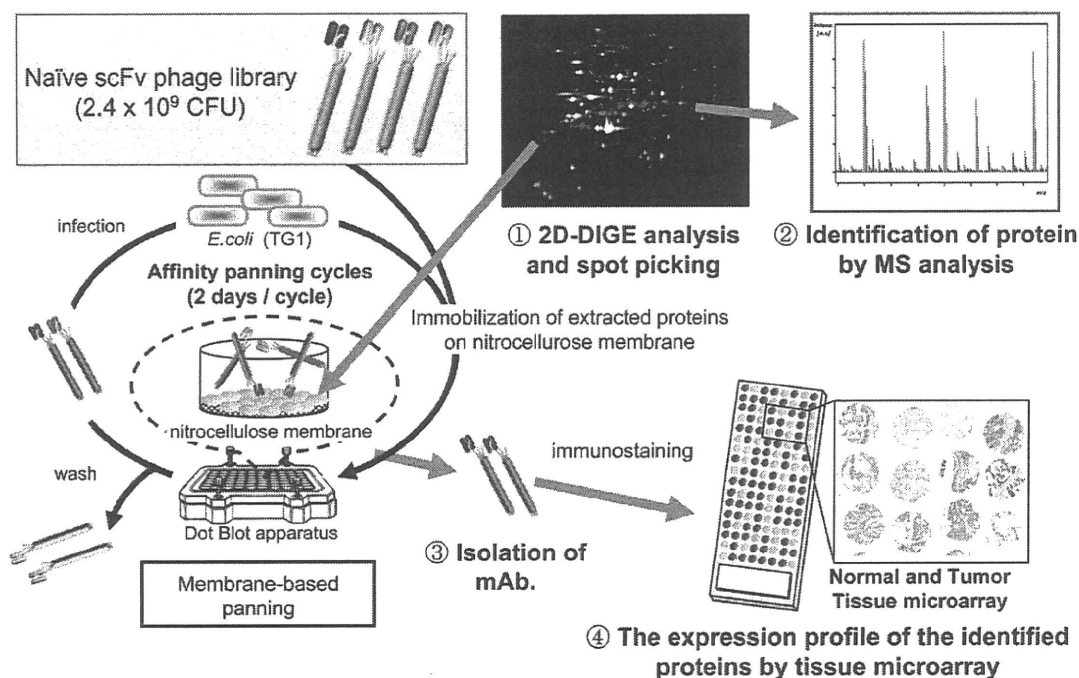


**Fig. 4.** Schematic illustration of the antibody proteomics system. Antibody proteomics system is an efficient method for screening tumor-related biomarker proteins. Because this system involves the direct isolation of monoclonal antibodies from 2D-DIGE spots without preparation of recombinant proteins, it enables the discovery and validation of tumor-related biomarker proteins by TMA analysis using the isolated scFv antibody-expressing phages.

proteome analysis or the antibodies against these proteins may not detect the antigen on formalin-fixed paraffin-embedded tissues. By contrast, TRAIL-R2, Cytokeratin 8 and Eph receptor A10 were specifically-expressed in over 40% of breast cancer tissues. We confirmed the immunohistochemical staining image generated by scFv antibody-expressing phages displayed a similar pattern to that generated by IgG type commercial antibody (data not shown). Interestingly, the expression rates of TRAIL-R2, Cytokeratin 8 and Eph receptor A10 were higher than the existing breast cancer marker, Her-2 (only about 25%). Moreover, the expression rates of TRAIL-R2 and Eph receptor A10 (cell membrane proteins) in Her-2 negative cases were over 40% and in Her-2 positive cases over 60%. This data indicates that TRAIL-R2 and Eph receptor A10 are promising alternative target candidates for anti-Her-2 antibody therapy ineffective patients, at least in terms of the expression profile. Further work is required to analyze the function of these proteins in more detail. Furthermore, by checking antigen expression profiles against clinical information, the expression rate of Cytokeratin 8 and Eph receptor A10 was found to have increased during progression of the clinical symptoms. These observations indicate that Cytokeratin 8 and Eph receptor A10 are promising diagnostic marker candidates for assessing the aggressiveness of breast cancer.

Recently, an anti-TRAIL-R2 antibody has been developed as an anticancer drug [31–33]. Moreover, Cytokeratin 8 has gained considerable attention as a cancer aggressiveness diagnostic marker [34–36]. These results demonstrate that this technology is able to select well-known drug-target markers (i.e., TRAIL-R2) and diagnostic markers (i.e., Cytokeratin 8) as well as unknown biomarker protein candidates (Eph receptor A10) from a large variety of differentially expressed proteins in cancer cells.

Our method employs a set of techniques for efficiently identifying biomarker candidates. Specifically, the method entails: 1) searching for differentially expressed proteins in disease samples, 2) identification of the proteins, 3) high throughput isolation of monoclonal antibodies against the proteins using a naïve scFv phage library, and 4) validation of the proteins by TMA analysis. This methodology is referred to as an "antibody proteomics system" (Fig. 4). We believe that the proteins identified using this approach will contribute to the drug development process. Indeed, the antibody proteomics system could become a platform technology for seeking tumor-related biomarker proteins by a proteomics-based approach.

## 5. Conclusions

In this study, we established the antibody proteomics system for efficiently screening and validating tumor-related biomarker proteins of interest by isolating specific antibodies directly from small amounts of proteins obtained via 2D-DIGE analysis. Applying this technique to the identification of breast tumor-related biomarker proteins, the expressions of Eph receptor A10, TRAIL-R2 and Cytokeratin 8 in breast tumor tissues were successfully validated from a large number of candidates. These results demonstrate that our original technology is an efficient and useful method for screening tumor-related biomarker proteins. Moreover, Eph receptor A10, TRAIL-R2 and Cytokeratin 8 identified in this study are promising breast tumor biomarkers for drug development.

## Appendix

Figure with essential color discrimination. Figs. 2–4 in this article have parts that are difficult to interpret in black and white. The full color images can be found in the on-line version, at doi:10.1016/j.biomaterials.2010.09.030.

## References

[1] Hanash S. Disease proteomics. Nature 2003;422(6928):226–32.
[2] Kavallaris M, Marshall GM. Proteomics and disease: opportunities and challenges. Med J Aust 2005;182(11):575–9.
[3] Oh-Ishi M, Maeda T. Disease proteomics of high-molecular-mass proteins by two-dimensional gel electrophoresis with agarose gels in the first dimension (Agarose 2-DE). J Chromatogr B Analyt Technol Biomed Life Sci 2007;849(1–2):211–22.
[4] Chaga GS. Antibody arrays for determination of relative protein abundances. Methods Mol Biol 2008;441:129–51.
[5] Kaufmann H, Bailey JE, Fussenegger M. Use of antibodies for detection of phosphorylated proteins separated by two-dimensional gel electrophoresis. Proteomics 2001;1(2):194–9.
[6] Xu ZW, Zhang T, Song CJ, Li Q, Zhuang R, Yang K, et al. Application of sandwich ELISA for detecting tag fusion proteins in high throughput. Appl Microbiol Biotechnol 2008;81(1):183–9.
[7] Au NH, Gown AM, Cheang M, Huntsman D, Yorida E, Elliott WM, et al. P63 expression in lung carcinoma: a tissue microarray study of 408 cases. Appl Immunohistochem Mol Morphol 2004;12(3):240–7.
[8] de Jong D, Xie W, Rosenwald A, Chhanabhai M, Gaulard P, Klapper W, et al. Immunohistochemical prognostic markers in diffuse large B-cell lymphoma: validation of tissue microarray as a prerequisite for broad clinical applications (a study from the Lunenburg Lymphoma Biomarker Consortium). J Clin Pathol 2009;62(2):128–38.
[9] Kozarova A, Petrinac S, Ali A, Hudson JW. Array of informatics: applications in modern research. J Proteome Res 2006;5(5):1051–9.
[10] Rimm DL, Camp RL, Charette LA, Costa J, Olsen DA, Reiss M. Tissue microarray: a new technology for amplification of tissue resources. Cancer J 2001;7(1):24–31.
[11] Tawfik El-Mansi M, Williams AR. Validation of tissue microarray technology using cervical adenocarcinoma and its precursors as a model system. Int J Gynecol Cancer 2006;16(3):1225–33.
[12] Asadi A, Pourfathollah AA, Mahdavi M, Eftekharian MM, Moazzeni SM. Preparation of antibody against horseradish peroxidase using hybridoma technology. Hum Antibodies 2008;17(3–4):73–8.
[13] Hadas E, Theilen G. Production of monoclonal antibodies. The effect of hybridoma concentration on the yield of antibody-producing clones. J Immunol Methods 1987;96(1):3–6.
[14] Makonkawkeyoon L, Pharephan S, Makonkawkeyoon S. Production of a mouse hybridoma secreting monoclonal antibody highly specific to hemoglobin Bart's (gamma4). Lab Hematol 2006;12(4):193–200.
[15] McKinney KL, Dilwith R, Belfort G. Optimizing antibody production in batch hybridoma cell culture. J Biotechnol 1995;40(1):31–48.
[16] Barbas 3rd CF, Kang AS, Lerner RA, Benkovic SJ. Assembly of combinatorial antibody libraries on phage surfaces: the gene III site. Proc Natl Acad Sci U S A 1991;88(18):7978–82.
[17] Coomber DW. Panning of antibody phage-display libraries. Standard protocols. Methods Mol Biol 2002;178:133–45.
[18] McCafferty J, Griffiths AD, Winter G, Chiswell DJ. Phage antibodies: filamentous phage displaying antibody variable domains. Nature 1990;348(6301):552–4.
[19] Okamoto T, Mukai Y, Yoshioka Y, Shibata H, Kawamura M, Yamamoto Y, et al. Optimal construction of non-immune scFv phage display libraries from mouse bone marrow and spleen established to select specific scFvs efficiently binding to antigen. Biochem Biophys Res Commun 2004;323(2):583–91.
[20] Smith GP. Filamentous fusion phage: novel expression vectors that display cloned antigens on the virion surface. Science 1985;228(4705):1315–7.
[21] Vaughan TJ, Williams AJ, Pritchard K, Osbourn JK, Pope AR, Earnshaw JC, et al. Human antibodies with sub-nanomolar affinities isolated from a large non-immunized phage display library. Nat Biotechnol 1996;14(3):309–14.